5-3-2008

A study of translunar trajectories for a small satellite navigation and communications mission

Christopher Matthew Becker

A STUDY OF TRANSLUNAR TRAJECTORIES FOR A SMALL SATELLITE NAVIGATION AND COMMUNICATIONS MISSION

By

Christopher Matthew Becker

A Thesis
Submitted to the Faculty of
Mississippi State University
in Partial Fulfillment of the Requirements
for the Degree of Master of Science
in Aerospace Engineering
in the Department of Aerospace Engineering

Mississippi State, Mississippi

May 2008

A STUDY OF TRANSLUNAR TRAJECTORIES FOR A SMALL SATELLITE NAVIGATION AND COMMUNICATIONS MISSION

By

Christopher Matthew Becker

Approved:

Carrie D. Olsen Assistant Professor of Aerospace Engineering (Director of Thesis)	Gregory D. Olsen Assistant Professor of Aerospace Enginering (Committee Member)
Ming Xin Assistant Professor of Aerospace Engineering (Committee Member)	Pasquale Cinnella Professor of Aerospace Engineering Graduate Coordinator for Aerospace Engineering

Wilbur G. Steele
Interim Dean
Bagley College of Engineering

Name: Christopher Matthew Becker

Date of Degree: May 2, 2008

Institution: Mississippi State University

Major Field: Aerospace Engineering

Major Professor: Dr. Carrie D. Olsen

Title of Study: A STUDY OF TRANSLUNAR TRAJECTORIES FOR A SMALL SATELLITE NAVIGATION AND COMMUNICATIONS MISSION

Pages in Study: 73

Candidate for Degree of Master of Science

Analysis was done to determine fuel optimal translunar trajectories from Earth geostationary transfer orbit to a specified target lunar orbit for a small satellite navigation and communication mission. The study included the optimization of impulsive and finite burn transfers. The inclusion of finite burns was necessary due to the low thrust nature of a small satellite propulsion system. Finite burn optimization was achieved using suboptimal parameterization control theory. The orbital parameters of the initial Earth orbit as well as the target lunar orbit were varied to see how this affected the optimal transfer results. Additionally, two engine thrust levels were explored to find the impact on the fuel mass required. All optimization analyses were completed using Copernicus, a trajectory optimization software package developed at the University of Texas at Austin for the National Aeronautics and Space Administration (NASA).

ACKNOWLEDGEMENTS

The author expresses his gratitude to the faculty and staff of the aerospace engineering department that made this thesis possible. They helped create an enjoyable and productive environment for the author during his six years at Mississippi State. A special thanks is given to Dr. Carrie Olsen, the thesis advisor, for all the help she offered during the course of the research described in this document. Gratitude is also expressed towards the other members of the thesis committee, Dr. Gregory Olsen and Dr. Ming Xin.

TABLE OF CONTENTS

LIST OF TABLES

LIST OF FIGURES

CHAPTER I

INTRODUCTION

In January of 2004, President Bush announced the Vision for Space Exploration.[1] This program laid out the future goals of the U.S. space program. Among these goals was to return humans to the Moon before 2020. These missions will not visit the Moon's surface for short stays like those of the Apollo missions, but they will establish permanent outposts on the lunar surface. To facilitate this goal, more detailed knowledge must be attained about the Moon and its environment. This task will fall to robotic precursor missions, such as the Lunar Reconnaissance Orbiter (LRO), that will be launched in the coming years.

In addition to mapping and surveying the surface of the Moon and determining more about its composition, a system must be established to communicate with and provide navigational assistance to lunar bases and other lunar orbiters. One way to meet this need is to place one or more navigation and communication satellites in lunar orbit. These satellites would act as relays between the astronauts and assets on the surface of the Moon and in lunar orbit and the mission controllers back on Earth. The more satellites placed in lunar orbit for this task, the more complete the coverage provided by this system will be. A small constellation could offer global coverage of the moon and allow for wide exploration of its surface by manned missions.

All the aspects of the new vision for the future of NASA must be funded with a limited budget. To do this, the available funds must be used as efficiently as possible. Traditional satellites are large and complex, and therefore they are very costly. Unless NASA's budget is expanded considerably, it will not be possible to field a sizeable lunar constellation of navigation and communication satellites and still be able to fund the lunar exploration program as well as all the other responsibilities assigned to NASA.

To lower the cost of a constellation, NASA could make use of low-cost small satellites. The concept of small satellites not only relates to their physical size, but also to the way in which they are designed and used. A typical definition of a small satellite is a spacecraft with a mass of 500 kilograms or less. These spacecraft are usually designed to complete one mission and do not have multiple instruments or payloads. This simplicity leads to lower costs to design and build the spacecraft and also to operate them. The concepts of small satellite design will be reviewed in Chapter 2.

Mississippi State University (MSU), in collaboration with Surrey Satellite Technology Limited (SSTL) of the United Kingdom, has proposed to NASA to design and develop a navigation and communications small satellite to be launched to the Moon in the 2012 timeframe.[2] This mission would be a testbed for the small satellite communication concept. If successful, it could lead to a constellation of such spacecraft to support manned operations once they begin around 2020.

The goal of this thesis is to explore the transfer trajectories that could be employed by a small satellite to travel from Earth orbit to its design mission orbit around the Moon. Because of its small size, a small satellite will have a similarly small propulsion system. This system will be relatively low thrust, compared to larger

spacecraft such as LRO. Therefore, any sizeable orbital maneuvers completed by a small satellite, such as those required to leave the vicinity of the Earth and travel to the Moon, could not be assumed to be impulsive. A lower thrust system will require longer periods of burn to get the same result as a high thrust propulsion system, and therefore gravity losses will be a significant factor.

This thesis examines translunar trajectories using both impulsive burns and finite burn arcs to find optimal transfers. The optimization was completed using Copernicus, a trajectory design optimization software package developed at the University of Texas at Austin for NASA. This package allows for the modeling of a wide variety of orbit and trajectory types including lunar and interplanetary transfers. Further detail about Copernicus will be provided in Chapter 2.

The impulsive transfer optimizations were done in the preliminary stages of this study to familiarize the writer with both Copernicus and the details of the lunar transfer problem. The methods employed and the results will be discussed in Chapter 3. Finite burn optimizations were then completed because they more accurately reflect a realistic transfer, specifically for a low thrust propulsion system. These optimizations are discussed in Chapter 4. Finally, phased finite transfers were examined. These transfers minimize the duration of any single engine burn by employing several perigee burns to gradually transfer from Earth to lunar orbit. Phased transfer results are presented in Chapter 5.

Design of the initial Earth orbit and the final lunar orbit used for all trajectory analyses is not within the scope of this thesis. The initial Earth orbit is mostly dictated by the capabilities of available launch vehicles. The choice of target lunar orbit is a function

of the mission to be completed as well as the dynamics of the lunar gravity field. For this study, a particular class of lunar orbits were selected and used as the targets for the transfer orbits. The particular Earth and lunar orbits and the rationale for these choices will be explained in Chapter 2.

In the final chapter, the conclusions obtained from the results of this study will be presented. Details of potential further research to expand on the results of this thesis will also be discussed.

CHAPTER II

BACKGROUND

The following subsections present the background information necessary to complete the research detailed in this thesis. These sections include a review of the Moon and its orbit around the Earth, an overview of the small satellite concept, the rationale for the choice of target lunar orbit as well as the type of translunar trajectory to be studied, and a brief description of the Copernicus optimization software package used to complete this thesis.

Moon's Orbit

The common point of view is that the Moon orbits around the Earth. For initial approximations, the Moon can be assumed to orbit the Earth in a circular orbit with a radius of 384,400 km. While this is a good approximation for any initial design or calculations, the true nature of the orbit of the Moon must be examined if more precise calculations are to be attempted. The Moon and the Earth actually orbit around their common center of mass, or barycenter, which is itself in orbit around the Sun. This relationship with the Sun is essential in understanding the actual behavior of the Moon's orbit.

The Earth orbit plane, in which the Earth orbits the Sun, is known as the ecliptic plane. It is useful therefore to reference the Moon's orbit around the Sun with respect to

the ecliptic plane. The Moon's inclination with respect to the ecliptic plane varies with a mean value of approximately 5.13 degrees. However when planning a translunar trajectory, it is more useful to model the behavior of the Moon with respect to an Earth-centered frame such as an IJK Earth-Centered Initial (ECI) frame. With respect to an ECI frame, the Moon orbits at an inclination that varies periodically on an 18.6 year cycle.

This variation is due to the location of the Moon's orbit with respect to the ecliptic. The Moon's node location changes due to solar perturbations. When the Moon's ascending node coincides with the vernal equinox, the Moon's inclination in the ECI frame is at its maximum with a value of approximately 28.58 degrees. Conversely, the inclination of the Moon is at its minimum when the Moon's descending node is in the direction of the vernal equinox resulting in an inclination of 18.32 degrees. Therefore any trajectory to the Moon will depend on where the Moon is in this 18.6 year cycle.

The eccentricity of the Moon's orbit in the ECI frame is approximately 0.0549. This results in a perigee radius of 363,300 km and an apogee radius of 405,500 km. Assuming the orbit to be circular would therefore introduce significant error for precise trajectory calculations. The orbital period of the Moon about the Earth is 27.317 days with up to a seven hour variation due to solar perturbations. Additionally, the argument of perigee (AoP) of the Moon's orbit rotates in the same direction as the Moon's orbital motion on an 8.9 year cycle. All of these described effects make the availability of a detailed lunar ephemeris mandatory for any lunar mission.[3]

Moon's Characteristics

Although the study described in this thesis is mainly concerned with the transfer from Earth orbit to lunar orbit, it would be helpful to describe the characteristics of the Moon, particularly its gravity field, as they are important to the rationale for the choice of target lunar orbit. If the Moon is assumed to be a point mass, the important features that will determine the orbit of spacecraft around the Moon are the radius of the Moon and its mass. The size or radius of the Moon is important to determine the minimum distance that a spacecraft can orbit the Moon's center, and the mass is likewise important because it determines the gravitational parameter, μ, of the Moon. The average radius of the Moon has been found to be 1738 km.[4]

The mass of the Moon can be determined using several methods. Early estimates were found by observing the effect of the Moon's gravity on the orbit of the Earth. This change in the Earth's orbit can be referenced to a nearby object such as the Sun. Using this method, the Earth to Moon mass ratio was determined to be approximately 81.33. Likewise, the Moon's mass can be determined by monitoring the effect of the Moon on spacecraft that pass near to or orbit it. By observing the behavior of the Mariner interplanetary spacecraft and the Ranger lunar impact spacecraft, the Earth/Moon mass ratio was further refined to 81.3.[4] This mass fraction leads to a lunar gravitational parameter of 4902.799 km^3/s^2.[5]

This value of the Moon's gravitational parameter is sufficient for two-body analysis of a spacecraft's orbit around the Moon, but depending on the characteristics of the orbit, there may be significant perturbations due to the Earth and Sun as well as the non-spherical nature of the Moon's true gravity field and the presence of significant mass

concentrations inside the lunar body. The Moon is constantly bombarded by meteors and other space debris and always has been. Without an atmosphere like the Earth's, these objects do not burn up but instead impact the surface. Because of this, the Moon's shape and density significantly deviate from that of a perfect point mass sphere. Another factor that contributed to the non-spherical shape of the Moon was its past and the nature of its formation.

Currently, the most accurate way to determine the specifics of the gravity model of the Moon is to monitor the behavior of spacecraft in lunar orbit. Using ground tracking stations on the Earth, tracking data is collected to analyze the deviations of the spacecraft with respect to the expected two-body orbit. This requires line of sight between the orbiting spacecraft and the Earth, so to date there is no direct information on the gravity model of the far side of the Moon. Far side gravity data can only be extrapolated by analyzing the long term trends of the orbit of lunar satellites.[6] The current Japanese lunar mission, SELENE, will make use of a relay satellite to enable collection of gravity field information for the far side of the Moon.

Some of the most recent gravity models have been compiled from the tracking data collected by the Lunar Prospector (LP) mission in 1998-1999. The LP mission led to the creation of the LP75, LP100, and LP165 models. The LP75 models were created before the end of the LP mission and therefore incorporate tracking data only from the nominal mission orbit of 100 km average altitude. The LP100 models were developed later and incorporated data collected during the extended mission of LP during which the altitude was decreased first to 40 km and then further to 30 km. The gravity data was further refined in the LP165 model which is complete to degree 122 with the further

gravity coefficients determined statistically using the 122 degree data as *a priori* knowledge. This process created reasonably accurate values for the coefficients up to order and degree of 110, with the remaining coefficients showing considerable noise. However, application of the LP165 model significantly increases the computational demand compared to the LP100 model.[6]

Small Satellites

In addition to the physical size difference between small satellites and conventional large satellites, there are also differences in their design philosophies and operations concepts. These differences lead to lower cost which is desirable by all parties involved in a satellite mission. A typical large satellite mission may have more than one objective and therefore possibly multiple payloads or instruments. This multi-tasking not only increases the complexity of operations, but it also requires larger support systems onboard the spacecraft. This overall complexity leads to larger costs than a simpler design which may only complete one mission task. Because of these high costs, the risk of a critical system failure that can endanger the entire mission is particularly undesirable. To safeguard against these possible failures, redundancy of critical spacecraft subsystems is typical. Again this causes an increase in the cost of the spacecraft.

The desire to avoid unnecessary risk is not unique to large spacecraft. Although small satellites are comparatively cheap compared to their larger counterparts, they are still sizeable investments on the order of tens of millions of dollars. Small satellite operators desire successful mission completion as much as large satellite operators. But small satellite designs permit a certain amount of risk while offering the opportunity to

gain greater functionality. Small satellites generally make use of commercial-off-the-shelf (COTS) hardware which may not have been designed specifically for space applications. Often these COTS components have superior functionality, such as higher clock speeds for computer components. These greater abilities can be advantageous to mission success, and the corresponding risks can be avoided or at least controlled if untested COTS technology is employed in a safe manner.[7]

One way to control the risks of using new hardware or software that has no previous flight experience is to use a tiered approach. The new technology is employed alongside less risky hardware with flight heritage instead of completely replacing it. Therefore, if the new technology does not function as desired, it will not endanger completion of the spacecraft's mission. The older technology can still complete the mission. SSTL uses this approach when it decides to use a new piece of hardware that it has not previously flown on a mission. The heritage equipment ensures that the mission can be completely successfully, but the new equipment, such as a higher resolution camera or imager, would produce more detailed results that would allow for more than the sufficient detail needed for mission success.[8] This allows the newer hardware to get flight heritage without endangering the current mission.

Another technique employed by small satellite missions is operational autonomy. Operations is a large mission cost driver that is often overlooked. By designing spacecraft that can operate autonomously for long periods of time, the need to have a human in the loop, constantly monitoring telemetry from the spacecraft, can be eliminated. If a mission critical failure or emergency does occur, the autonomous systems can alert human operators of the problem. The integration of autonomy into the

spacecraft systems may require larger upfront costs, but the overall mission cost will decrease because of the lower human staffing requirement. And, if a spacecraft is "simple", it can be more easily "safed" until a human can be called in to fix the problem.

In summary, small satellites have many benefits that may allow them to replace or complement larger spacecraft. Their small size allows them to launch on a variety of launch vehicles, often at a decreased cost as a "piggyback" mission. The decreased overall spacecraft cost allows more organizations to employ the use of satellites, and in the case of the lunar mission of interest to this thesis, they may allow the deployment of a constellation of satellites instead of one or two traditional spacecraft. Finally, because of their lower level of complexity, the time from design to launch and operation is on the order of one to two years compared to the much longer lead time of larger spacecraft.[7]

Choice of Earth and Lunar Orbits

The focus of this study is the optimization of transfers from Earth to lunar orbit. Limited research was done on the specific benefits of one choice of Earth or lunar orbit over another as this was outside of the scope of this study. However it is important to choose suitable orbits as they do have an effect on the fuel and transfer time requirements of the translunar transfer. In this sub-section, the rationale for the choice of both the initial Earth orbit and the final target lunar orbit will be explained.

To reduce the requirements of the spacecraft onboard propulsion system, it is desirable to launch the spacecraft into as large of an orbit as possible. The size and orientation of this orbit is dictated by the abilities of the chosen launch vehicle as well as any launch site restrictions such as launch azimuth. In the course of preliminary studies

conducted by the MSU/SSTL team, the initial choice of launch vehicle was the Indian Space Research Organization PSLV-XL.[9] This choice was based on the payload mass capabilities of the launcher as well as the relatively low cost of the launcher. The PSLV can launch an estimated 1200 kg payload to geostationary transfer orbit (200 x 35786 km altitude) and can place spacecraft at inclinations ranging from 18 to 100 degrees.[10] This payload mass performance is sufficient for the current design mass estimate of the proposed lunar small satellite. Therefore, this geostationary transfer orbit (GTO) was used as the baseline initial Earth orbit for all translunar trajectory optimizations.

The choice of target lunar orbit is heavily dependent on the specifics of the satellite mission. NASA's current plans are for a manned lunar base to be built at the southern lunar pole where there is evidence of possible frozen water. Therefore it would be ideal for any navigation/communication satellite to spend as much of its orbit over this region as possible. Although there are several options that may meet these requirements, the option chosen was a highly elliptical orbit with its apoapsis over the southern pole. Specifically, the initial design point for the lunar orbit was a frozen orbit selected from a class of such orbits developed by Todd Ely.[11] His study focused on finding frozen orbits that would be suitable for communications relay satellites to communicate with the region around the southern lunar pole. The use of a frozen orbit would decrease the orbit maintenance requirements and therefore the necessary fuel required, which is of particular interest to the current small satellite proposal. The orbital elements of the frozen orbit of interest are shown below in Table 1. This orbit yields stable librations in the eccentricity – argument of periapsis space.

Table 1

Lunar Frozen Orbit (Ely)[11]

Semi-major Axis	6541.4 km
Eccentricity	0.6
Inclination	63.01 deg
Right Ascension of the Ascending Node	0 deg
Argument of Periapsis	90 deg

Translunar Trajectories

A translunar trajectory is an orbit employed to transfer a spacecraft from the Earth to the Moon. These trajectories can take many forms depending on the requirements of a particular mission. The general categories of transfers include direct, bi-elliptic, low thrust spiral, and weak stability boundary (WSB) transfers. A brief description of each of these four types is given in the following pages.

As the name implies, direct transfers are the simplest and have the shortest transfer time of the four categories. These transfers are Hohmann-like and place a spacecraft on a transfer ellipse with periapsis near Earth and apoapsis in the vicinity of the Moon. An example of this type of transfer is shown in Figure 1. The transfer begins with a translunar injection (TLI) burn that places the spacecraft into the transfer orbit. Once the spacecraft reaches the Moon, a lunar orbit injection (LOI) burn is performed, typically near the perilune point, to place the spacecraft into lunar orbit. The TLI burn can be performed directly at launch, or the launch vehicle can place the spacecraft into a temporary parking orbit around the Earth followed later by the TLI maneuver. This parking orbit can be used for spacecraft checkout before translunar injection or as a coast period for the spacecraft and the Moon to reach the proper alignment for the transfer.

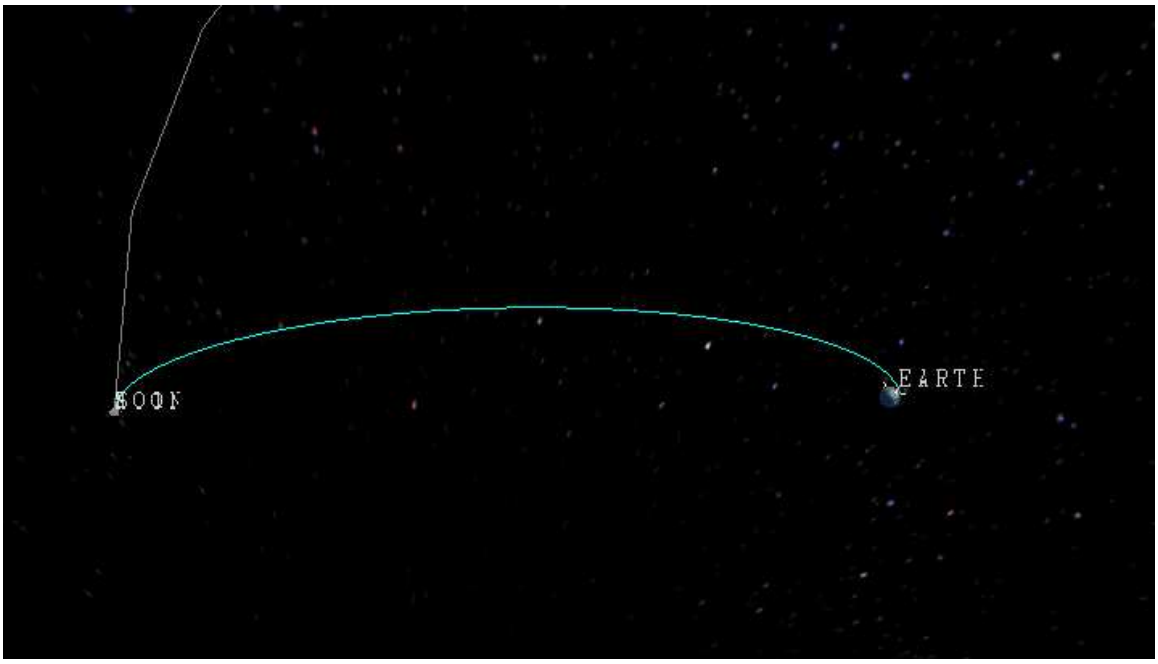

Figure 1

Direct Earth to Moon Transfer (Copernicus screenshot)

Because direct transfers are usually the shortest in total transfer time, they are the most expensive in terms of propulsive requirements. Therefore the fuel mass will be a larger fraction of the total spacecraft mass resulting in lower available payload mass. But the benefit of shorter transfer time may outweigh this disadvantage for certain missions. The shorter transfer time will result in lower operations costs as well as a shorter period of exposure of the spacecraft to the space environment. This is particularly beneficial for manned missions as it also decreases the life support mass requirements for items such as food, water, and oxygen.

Since the orbit of the spacecraft must be raised so that it intersects the Moon's orbit at some point, it is difficult to decrease the TLI requirement beyond a particular lower limit. However, the propulsive requirements of the transfer can be decreased by

reducing the Δv requirement of the LOI burn. This is the goal of a weak stability boundary (WSB) transfer. A WSB transfer makes use of the dynamics of the four body system composed of the Earth, the Moon, the Sun, and the spacecraft to capture into lunar orbit ballistically, that is without the need for an LOI maneuver or, at least, a significantly reduced one.

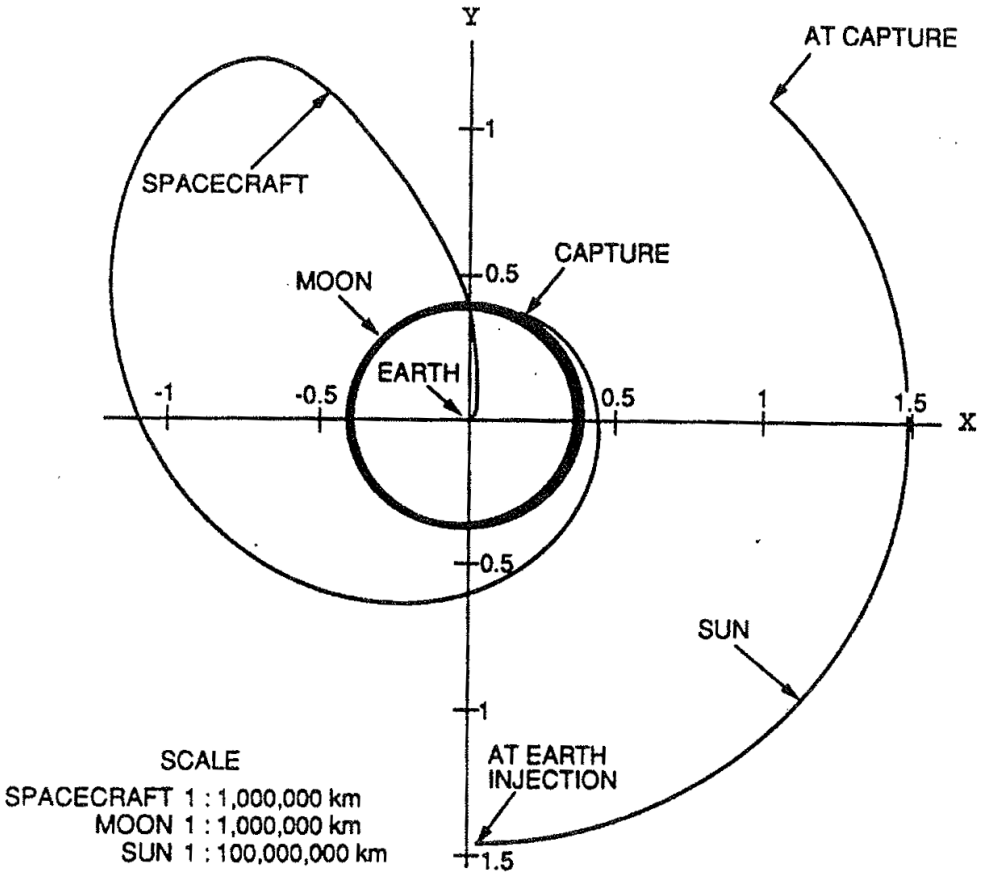

Figure 2

Weak Stability Boundary Transfer[12]

The general design of a WSB transfer is to place the spacecraft in a region well beyond the orbit of the Moon where it will experience perturbations due to the Sun.

Figure 2 shows an example of a weak stability boundary transfer. The effect of the solar perturbations is to increase the angular momentum of the spacecraft's orbit. This increase in angular momentum is necessary to raise the periapsis of the spacecraft's orbit, with respect to the Earth, to the radius of the Moon's orbit around the Earth. To obtain the necessary increase in angular momentum, the spacecraft must loiter in the zone where it is affected by solar perturbations for a considerable amount of time.[12] According to preliminary studies conducted by SSTL, the total duration for the translunar transfer would be three to five months, which is considerably larger than the three to five day transfer time for a direct transfer.[13] Therefore the decrease in the LOI requirement may be offset by the increased operations cost for the transfer as well as harsher design requirements on the vehicle due to the longer duration of the mission, deep space navigation, increased radiation exposure, etc.

A third option is a bi-elliptic transfer, which is a compromise between the direct and WSB transfer methods. Unlike the direct Hohmann-type transfers that use a single transfer ellipse, a bi-elliptic transfer first places the spacecraft into an intermediate transfer ellipse. This intermediate ellipse has an apoapsis greater than that of the final target orbit. Once the spacecraft reaches apoapsis of the intermediate ellipse, another maneuver is completed to place the spacecraft into a second elliptical orbit with a periapsis that intersects the target orbit. Finally a third burn is completed to enter into the final orbit. Figure 3 shows a bi-elliptic transfer.

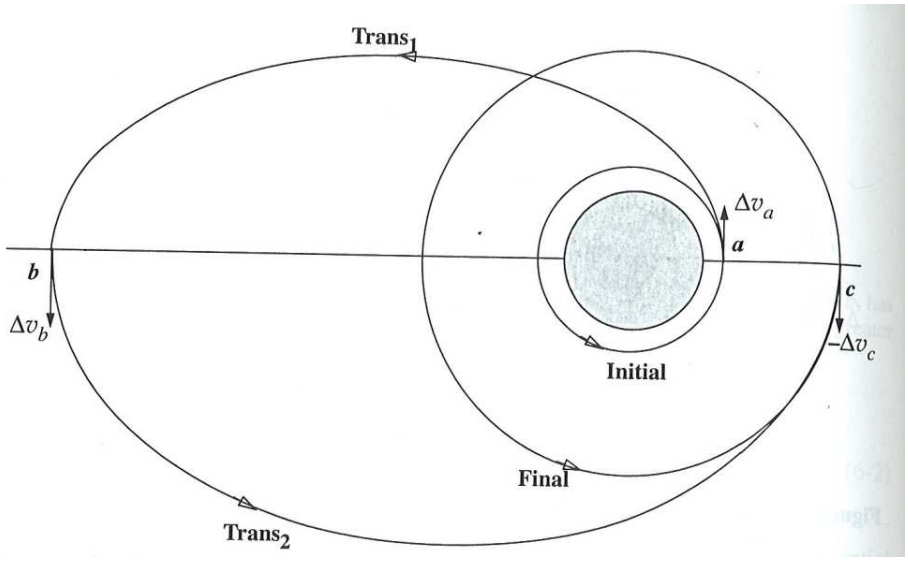

Figure 3

Bi-elliptic Transfer[5]

For certain cases, the bi-elliptic may be more efficient than a Hohmann transfer. The ratio, R, between the radii of the final and initial orbits is used to determine whether a bi-elliptic transfer is more efficient than a Hohmann transfer. This ratio results in three divisions. For the case of transfers between two circular orbits, if the ratio is between 0 and 11.94, the Hohmann transfer is more efficient. If the ratio is greater than 15.58, the bi-elliptic transfer may be more efficient, and if the ratio is between 11.94 and 15.58, further criteria is necessary to determine which method is superior. Figure 4 shows this behavior. R^* is the ratio of the radius of the final orbit over the radius of the initial orbit for the bi-elliptic transfers. The bi-elliptic transfer may decrease the total Δv, but it can result in a considerably longer flight time giving it the same disadvantages of the WSB transfer.[5]

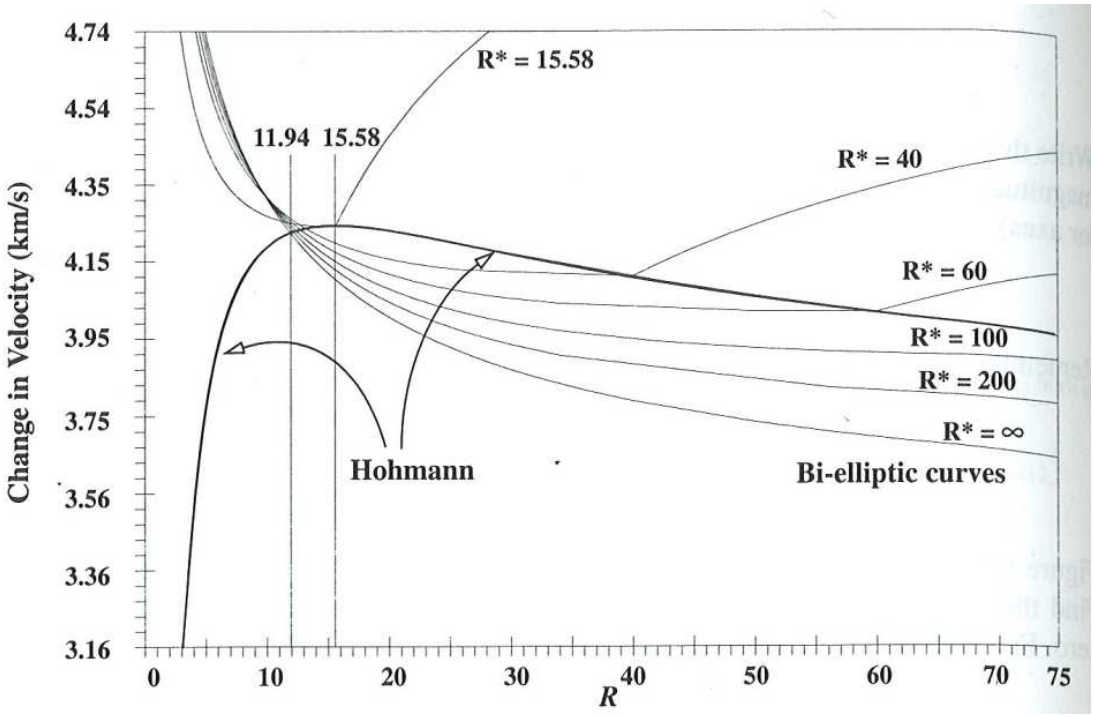

Figure 4

Delta V Requirement vs. Radius Ratio for Hohmann and Bi-elliptic Transfers[5]

The final major category of translunar transfer is a low thrust spiral trajectory. Spiral trajectories make use of low thrust, high specific impulse engines that can burn for extended periods of time to gradually increase the size of the spacecraft's orbit. One example of a mission that employed this type of transfer was the SMART-1 lunar mission. Such spiral trajectories make use of thrusting and coast periods designed using optimal control theory. Spiral trajectories are created using a specific type of engine such as an electric ion propulsion system. The inherent efficiency of such engines is, however, countered by the extremely long transfer times involved. These transfers take approximately eighteen months.[14] Figure 5 shows an example of this trajectory type.

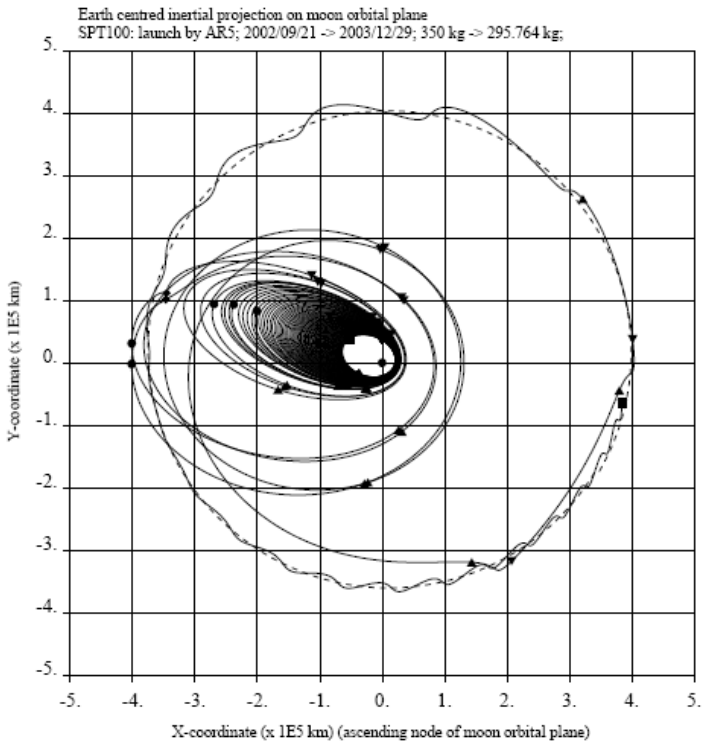

Figure 5

SMART-1 Transfer Trajectory[14]

For the purpose of this thesis, only direct transfers are examined. The specific transfers examined include one TLI burn transfers as well as multiple-burn phased transfers. A phased transfer separates the single large TLI burn into several smaller ones that gradually increase the apogee radius of the spacecraft's orbit until it intersects the Moon's orbit. This approach decreases gravity losses which are particularly significant for lower thrust engines, such as those typically used on small satellites. Such engines require a longer period of continuous thrusting to produce the same Δv as a higher thrust engine.

Copernicus

Copernicus is "a general trajectory design and optimization system"[15] developed at the University of Texas at Austin for NASA Johnson Space Center. It was developed as a tool that allows a user to model and optimize a wide variety of spacecraft trajectories ranging from simple Earth orbits to more complicated interplanetary trajectories.

Program Overview

The basic element of a trajectory in Copernicus is called a segment. A segment is a trajectory arc between two node points, an initial and final node. Between the node points, the trajectory of the spacecraft is propagated using the gravity model selected by the user.

At the initial and final node points the user specifies the current state of a spacecraft. This state is defined by time, mass, and orbital state parameters. The time of the segment is specified by providing exactly two of the following three time parameters: initial time (T0), time of flight (DT), and final time (TF). Providing two of these time parameters uniquely defines the third. The mass is defined by inputting the initial mass (M0) of the spacecraft at the beginning of a segment. Additionally, mass changes can be applied at nodes. These can be used to model actions such as detachment of a spent rocket stage or deployment of a satellite from the main spacecraft. Finally, the orbital state of the spacecraft at the beginning of a segment is specified using a variety of methods such as radius and velocity vector or classical orbital elements. The central body and coordinate frame can also be specified for each individual segment.

These time, mass, and orbital state variables can be used to model a simple non-powered trajectory arc, but more complicated trajectories can be modeled by applying maneuvers at the node points or along the segment arc. Impulsive maneuvers can be modeled at either node point while finite burns are applied to the segment arc itself. Impulsive burns are modeled by defining either the specific impulse or exhaust velocity of the propulsion system and the direction of the burn. Various reference frames for the maneuver can be specified, such as central body-centered or spacecraft body-centered frames.

Finite burn maneuvers are applied to the entire length of a segment arc. These maneuvers are first defined by choosing an optimization model. Copernicus provides two options: suboptimal control parameterization or optimal control theory. The specifics of these two methods will be explained in a later section. After an optimization model is chosen, the propulsion system is defined by specifying two of the following three parameters: engine thrust, specific impulse, and exhaust velocity. Next the direction of the burn is specified using different variables depending on the burn model chosen. This description will concentrate on the sub-optimal control options because that was the method chosen to complete this thesis. The initial direction of the finite burn is specified using the angles α_0 and β_0, where α_0 defines the direction in the X-Y plane of the chosen coordinate system, and β_0 defines the out-of-plane direction. If the burn is specified using only these two parameters, the direction of the burn will not change. However first and second time derivatives, of these values can be defined, so that the direction of the burn will change with time according to the following relationship (Eq. 2-

1), where $\dot{\alpha}$ and $\ddot{\alpha}$ are the first and second time derivates of α_0 and t and t_0 are the current and initial times respectively. This equation governs the behavior of α_0

$$\alpha(t) = \alpha_0 + \dot{\alpha}_0 \cdot (t - t_0) + 0.5 \cdot \ddot{\alpha}_0 \cdot (t - t_0)^2 \quad (2\text{-}1)$$

with an analogous equation governing the behavior of β_0.[15]

Once a segment is defined it can be used by itself or it can be connected to other segments to model an entire mission or complex maneuver sequence. To connect segments, state variables can be set it "inherit" the values from other segments. For example, to set one segment to follow a first segment, the initial time, mass, and orbital state variables would be set to inherit the final values of the previous segment.

Any of the parameters examined so far, as well as others, can be set as optimization variables. By selecting an appropriate optimization and integration method, a trajectory can be optimized to minimize or maximize a cost function specified by the user. This cost function and any constraints are specified using segment functions. The segment functions allow the user to tell Copernicus what values any particular variable is allowed to take. This could be used, for example, to specify what the final orbital elements of a spacecraft's orbit must be after an orbit change maneuver. Also in the segment functions section, any parameter can be added to the objective function.

The most obvious advantage of Copernicus as an optimization program is its visualization options. Copernicus offers both two-dimensional and three-dimensional visualizations. These visualizations not only show the current state of any segments, but they also update in real time during the course of an optimization run. This allows the user to monitor Copernicus as it searches for optimal results. Therefore the user can

intervene and stop the process if an obvious error is detected. This is very helpful in detecting improperly defined problems.[15,16]

Finite Burn Methods

Unlike impulsive maneuvers which assume that a force is applied instantly, finite burn maneuvers apply a force over a finite period of time. It may be sufficient to model burns completed by high thrust propulsion systems as impulsive, but with a low thrust system, such as that onboard a small satellite, this will introduce significant error. For example, during an ideal Hohmann transfer, a Δv must be applied instantaneously at either the apoapsis or periapsis point of an orbit along the orbital velocity vector, but even for high thrust engines this is not actually physically possible. The maneuver will take place over some finite period of time. As time elapses, the spacecraft will move along its orbit and away from the apoapsis or periapsis point. Therefore losses will be introduced because the impulse applied to the spacecraft is no longer being imparted at the most efficient location in the spacecraft's orbit.

If the maneuver occurs over some finite period of time and therefore some finite distance along the spacecraft's orbit, it would be useful to determine the optimal direction in which to burn the engine. Copernicus has two methods for optimizing finite burns, suboptimal parameter optimization and optimal control theory. Suboptimal parameter optimization is a simplification of the very complex multidimensional boundary value problem that must be solved when applying optimal control theory. This suboptimal control results in a thrust vector that is "constrained to a limited set of functions"[17] such

as quadratic or sinusoidal. More complex behaviors can still be modeled using suboptimal control by chaining together a series of burn segments.

Optimal control theory deals with the minimization or maximization of a function of the following form (Eq. 2-2). Φ is a "scalar function representing a cost function that depends in general on the initial and final times and states."[17] The L function in the

$$J = \varphi(t_0, t_f, x(t_o), x(t_f)) + \int_{t_0}^{t_f} L(t, x(t), u_c(t))dt \tag{2-2}$$

integral is a function of time and the state vector, x, and control vector, u_c, which are themselves functions of time. The state vector contains the position and velocity of the spacecraft, while the components of the control vector would dictate the orientation of the propulsion system. Initial and final boundary conditions, such as the requirement to reach a certain position or orbit, can be used to constrain the function φ by adjoining them using Lagrange multipliers. This results in a new function given below (Eq. 2-3),

$$G(t_0, t_f, x_o, x_f, \xi) = \varphi(t_0, t_f, x(t_o), x(t_f)) + \xi^T \theta(t_0, t_f, x_0, x_f) \tag{2-3}$$

where ξ is a vector of Lagrange multipliers and θ represents the constraints. The time dependent scalar function L is then constrained by the dynamics of orbital motion in the following way (Eq. 2-4),

$$H(t, x, u, \lambda) = L(t, x, u) + \lambda^T f(t, x, u) \tag{2-4}$$

where λ is a time dependent vector of Lagrange multipliers and f is the function defining the orbital motion. Combining all of this results in the final form of the cost function, J^*, shown below (Eq. 2-5).[17]

$$J^* = G + \int_{t^0}^{t^f} (H - \lambda^T f)dt \tag{2-5}$$

The optimization using this complex cost function was not employed in the work of this thesis. Instead, the simpler suboptimal parameter optimization method was used. This simplification is allowable because the finite burns being modeled for the purposes of this thesis are relatively simple. The burns do not require complex thrust steering like what might be necessary for a low thrust spiral trajectory.

Optimization Method

The version of Copernicus used for this thesis offers eight algorithm choices that allow the user to target or optimize a given problem. The targeting algorithms allow the user to target boundary conditions but do not allow for optimization, so they are not useful for the purposes of this effort. The remaining optimization algorithms can be used to target as well as optimize a particular problem. Of the three optimization algorithms, two are for solving dense problems while the final one can solve sparse problems. For this work, the author chose the sparse SNOPTA optimizer.[15] SNOPTA is an interface for the SNOPT optimization system developed at the University of California, San Diego and Stanford University. SNOPT can be used to optimize both linear and nonlinear cost functions with both linear and nonlinear constraints. For problems with only linear functions, SNOPT uses a primal simplex method, a linear programming solution method.[18]

A linear programming problem will have the following form (Eq. 2-6), where $a_{k,i}$, b_k, and c_i are constants and X_i are the optimization variables. If the problem of interest

$$\min f(X) = \sum_{i=1}^{n} c_i X_i \qquad \text{(2-6)}$$

such that

$$h_k(X) = \sum_{i=1}^{n} a_{k,i} X_i = b_k$$

$$X_i \geq 0$$

has inequality constraints, these constraints are converted to equality constraints by introducing slack and surplus variables. These new variables simply become additional optimization variables. If the inequality constraints have the following form (Eq. 2-7),

$$\begin{aligned} g_j(X) &\leq b_j \\ g_j(X) &\geq b_j \end{aligned} \qquad \text{(2-7)}$$

then after the introduction of slack or surplus variables respectively, they will take on this form (Eq. 2-8), where a slack variable has been added to the less than or equal to

$$\begin{aligned} h_j(X) &= g_j(X) + s_j = b_j \\ h_j(X) &= g_j(X) - s_j = b_j \end{aligned} \qquad \text{(2-8)}$$

constraint and a surplus variable has been added to the greater than or equal to constraint. Like the original optimization variables, these slack and surplus variables are restricted to be non-negative. If there are optimization variables that are not sign-restricted, they are replaced in the following manner (Eq. 2-9), where X is the original optimization variable,

$$\begin{aligned} X &= X^+ - X^- \\ X^+ &\geq 0 \\ X^- &\geq 0 \end{aligned} \qquad \text{(2-9)}$$

and X^+ and X^- are now optimization variables that are restricted to be non-negative.[19]

The linear constraints will form a complex polyhedron in the n-dimensional design space, where n is the number of design variables. For a solution to be feasible, it

must lie on the boundaries of this polyhedron, and the optimal solution will occur at one of the vertices of the complex polyhedron. When the number of constraints, m, is greater than the number of optimization variables, n, feasible solutions are found by setting n minus m of the optimization variables to zero and solving for the remaining variables. The simplex method is then employed to move from each feasible solution to the next until the optimal solution is found.[19]

For problems involving nonlinear objective functions or constraints, SNOPT makes use of sequential quadratic programming (SQP). This method uses a series of quadratic programming (QP) subproblems. In each subproblem, the objective function and constraints are approximated in a form such as the following (Eq. 2-10), where L is

$$\min Q = \nabla f(X)^T \Delta X + 0.5 \Delta X^T (\nabla^2 L(X)) \Delta X \quad \text{(2-10)}$$
$$\text{such that}$$
$$h_m(X) + \nabla h_m{}^T \Delta X = 0$$

the Lagrange function of the original optimization problem, and the ∇ functions are the gradients of the objective function and the constraints.[19] Solving the QP subproblem may take several iterations. These iterations are referred to as minor iterations, while each QP subproblem is a major iteration of the SQP procedure. The result of each subproblem is a search direction towards the next major iterate.

The user can control the accuracy of the results of the SNOPT algorithm with a set of tolerance settings. The Major Optimality Tolerance controls the accuracy of the optimization variables associated with the equality constraints. The Major Feasibility Tolerance relates to the accuracy with which any nonlinear constraints are met. And finally the Minor Feasibility Tolerance sets the requirement on the tolerance to which the side bounds on the optimization variables should be met. The user can also specify other

options such as the maximum number of iterations of both the minor and major iterations.[15]

For the optimizations completed for this effort, the objective functions and the constraints are non-linear because of the nature of orbital mechanics. The objective function will either be the ΔV magnitude of required impulsive burns or the final mass of the spacecraft. The constraints are the orbital elements of either the transfer orbit or the target lunar orbit.

CHAPTER III

IMPULSIVE BURN TRANSFERS

Although the low thrust propulsion system of a small satellite implies that large orbital maneuvers cannot be modeled accurately as impulsive, impulsive burn analysis remains a good first step in to begin the translunar trajectory analysis. The impulsive burn model provides an excellent first estimate of the size of the maneuvers required as well as the general direction in which they need to be applied. Additionally, because of their relative simplicity compared to finite burn arcs, impulsive burn analysis was an instructive first use of the Copernicus software package.

The impulsive burn transfer optimization was done in stages to simplify the search space. The first step was to create a trajectory that intercepted the Moon. This was done by constraining the final radius of the transfer orbit to be zero with respect to the Moon. Therefore the trajectory would intersect the Moon at its center. During this step, the Moon is treated merely as a target with no gravity field of its own, so the presence of the Moon had no affect on the spacecraft's trajectory. The motion of the Moon was modeled using the JPL DE 405 ephemeris provided in Copernicus.

The initial Earth orbit of the spacecraft had the following orbital elements, shown in Table 2. The first optimizations were done assuming an inclination of 18 deg, the minimum allowable inclination from the PSLV launch site.[10] This would provide the largest boost from the Earth's rotation. After further input from SSTL[9], 90 deg

Table 2

Initial Earth Orbit

Semi-major Axis	24371 km
Eccentricity	0.73
Inclination	18 deg or 90 deg
Argument of Periapsis	90 deg

inclination orbits were also examined. The optimization variables were the initial time of the scenario, which allowed for the proper initial phasing with respect to the location of the Moon in its orbit, the duration of the transfer, the right ascension of the ascending node (RAAN) and true anomaly of the initial Earth orbit, and the magnitude of the TLI burn. All burns used a spacecraft-centered coordinate frame, called the VUW frame in Copernicus. In this frame, the X axis is in the direction of the spacecraft orbital velocity vector, the Z axis is in the direction of the orbital angular momentum vector, and the Y axis is in the orbit plane and completes a right-handed triad. The TLI burn was constrained to be tangential, or along the X axis, which is generally the most efficient type of burn. The objective function minimized for all impulsive burn transfers was the total ΔV magnitude of completed maneuvers.

Once this initial optimization had converged, the next step was to include the Moon's gravity and tune the transfer orbit so that it would have the proper orientation for insertion into the desired lunar orbit. For all impulsive burn optimizations, the Ely frozen orbit as defined in Table 1 was used as the target lunar orbit. The orientation was achieved by constraining the final conditions of the transfer orbit. The inclination and argument of periapsis were targeted to be that of the target lunar orbit. The radial velocity of the spacecraft with respect to the Moon was set to zero. This constraint places

the spacecraft at periapsis with respect to the Moon. And the final radius magnitude was restricted initially to be greater than 2615 km, the periapsis radius of the target lunar orbit, and less than 10000 km. This initial, coarse targeting was then refined by lowering the upper bound on the final radius to 5000 km. This final radius constraint ensured that the LOI burn would be completed near the periapsis of the target lunar orbit and not the apoapsis.

After the orbit orientation was successfully completed, the final step was to include and optimize the LOI burn. Unlike the TLI burn which was restricted to be along the spacecraft's orbital velocity vector, the LOI burn was free to occur in any direction in the orbit plane. Although the spacecraft's initial Earth orbit inclination was different than its final (Earth-equivalent) inclination once it entered lunar orbit, initial optimizations showed that the LOI burn did not require an out of plane component. The pull of the Moon's gravity as the spacecraft approaches the Moon actually affects the spacecraft's inclination. Therefore by entering the Moon's sphere of influence at an appropriate location, the spacecraft's inclination can be altered without the need for a propulsive maneuver. The addition of the LOI burn introduced two more optimization variables, the X and Y components of the LOI burn.

To obtain the target lunar orbit orbital elements precisely, it was often necessary to toggle the optimization variables on and off. This reduced the size of the search space. Once the solution began to converge towards the desired target, the disabled optimization variables could then be reactivated to further optimize the result. An example of an optimization variable that might be disabled is the initial start time of the scenario. This variable and the RAAN of the initial Earth orbit provide similar functions. Both can be

used to change the phasing of the spacecraft transfer orbit with respect to the Moon in its orbit. To obtain an initial feasible orbit, it was not always necessary to have them both as optimization variables. However, since the Moon's orbit is inclined with respect to the Earth's equatorial plane, changing the RAAN of the Earth orbit affects the declination of the Moon with respect to the Earth at the end of the transfer. So to ensure an optimal result, the initial time of the scenario was reactivated once the solution began to converge.

Although the impulsive burn optimizations were done by minimizing the total ΔV required, ΔV can be easily translated into fuel mass required. This relationship is given below (Eq. 3-1).[20] I_{sp} is the specific impulse of the engine, g is the gravitational

$$\Delta V = I_{sp} g \ln(\frac{M_i}{M_f}) \tag{3-1}$$

acceleration at the Earth's surface, and M_i and M_f are the initial and final mass of the spacecraft respectively.

The first impulsive burn transfers were completed using Ely's frozen orbit presented in Table 1 as the target lunar orbit, but the argument of periapsis was only restricted to be between 80 and 100 deg. Then the inclination of the lunar orbit was varied from 40 deg to 140 deg in 5 deg increments to see what effect this had on the total ΔV required. Finally, the argument of periapsis was varied from 60 to 120 deg, also in 5 deg increments, using a 90 deg target inclination. These optimization runs were completed for both the 18 deg and 90 deg inclination initial Earth orbits for a series of argument of perigee values. For the 18 deg orbit, argument of perigee values of 0, 90, 180, and 270 deg were explored. The 90 deg inclination orbit optimizations were

restricted to 0 and 180 deg argument of perigees because 90 and 270 deg argument of perigees place the line of apsides of the Earth orbit nearly perpendicular to the Moon's orbit. Any transfer using these initial orbit configurations would require a rotation of the line of apsides and would therefore be highly fuel prohibitive.

18 Degree Inclination Earth Orbit

The following figures show the results obtained from the 18 deg inclination GTO Earth orbit transfer optimizations. Figures 6 through 10 show the affect of target lunar orbit inclination on the final spacecraft mass and each of the optimization variables for the 0 deg argument of perigee initial Earth orbit case. Figure 6 shows a decrease in the final mass of the spacecraft as the inclination of the target lunar orbit increases. A larger final mass means a smaller ΔV is required. As the ΔV increases, more fuel is necessary resulting in a lower final mass. The initial mass of the spacecraft for all transfer cases was 1000 kg. Although there is an apparent rise in the fuel required with increasing inclination, the overall increase is not appreciable. Figure 7 shows the change in total transfer time. The transfer time increases with increasing lunar orbit inclination, with an overall increase of 8 hours from the 40 deg to 140 deg inclination orbit.

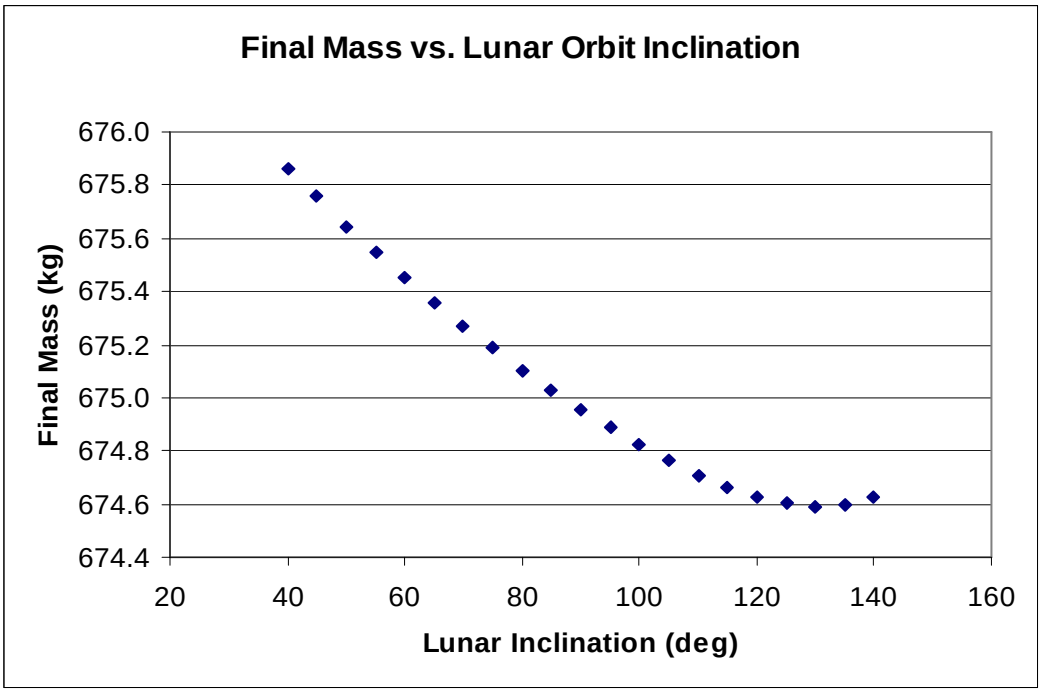

Figure 6

Final Spacecraft Mass vs. Lunar Orbit Inclination (18 deg inclination, 0 deg AoP GTO)

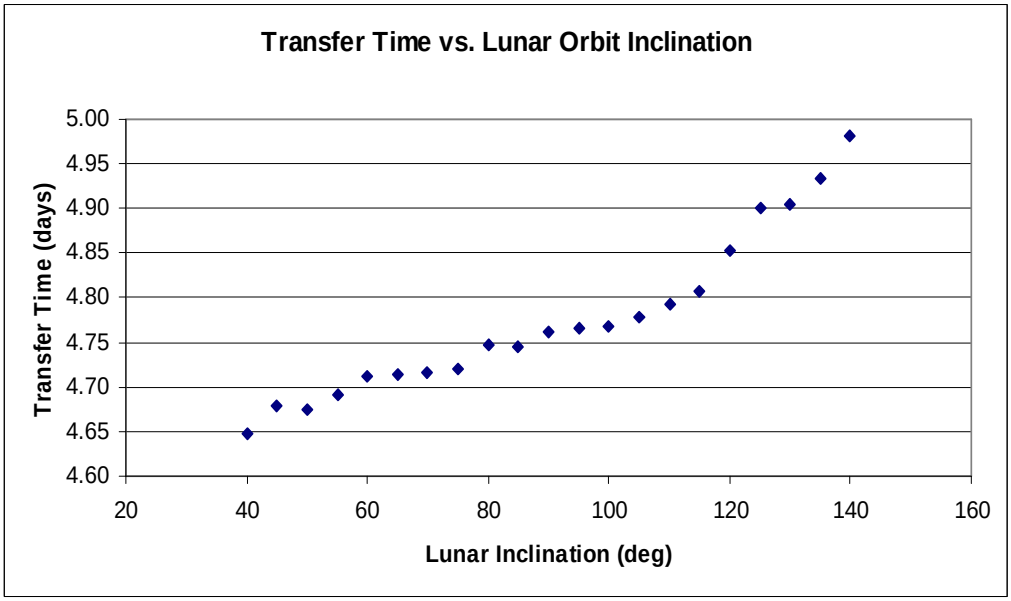

Figure 7

Transfer Time vs. Lunar Orbit Inclination (18 deg inclination, 0 deg AoP GTO)

Figure 8 shows the change in initial time with respect to lunar orbit inclination. The initial time is measured from the epoch time of the scenario, 12:00 GMT Jan 1 2012, to the time of the translunar injection. The lower inclination lunar orbits show a slightly later injection time than the higher inclination orbits.

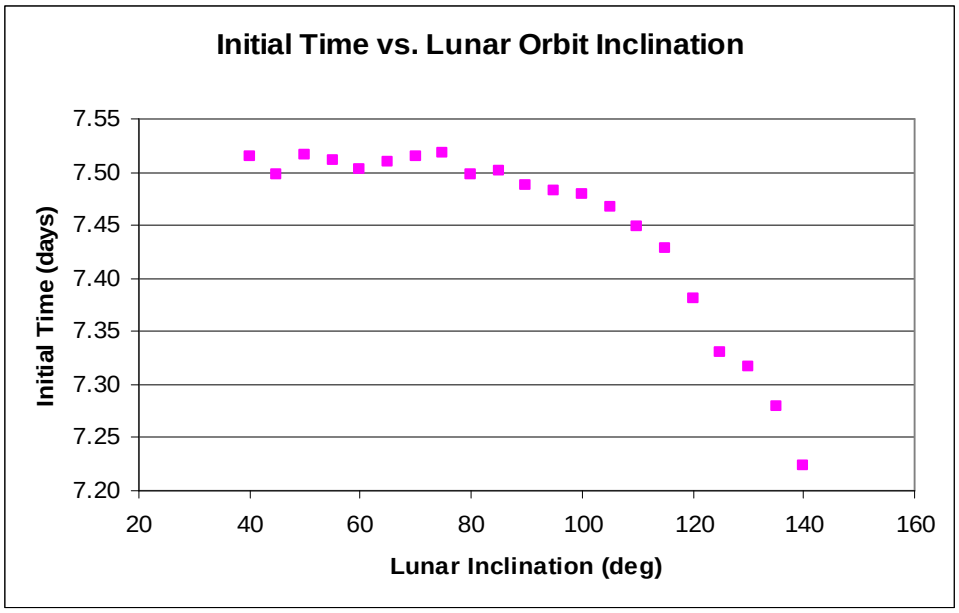

Figure 8

Initial Time vs. Lunar Orbit Inclination (18 deg inclination, 0 deg AoP GTO)

Figure 9 shows an increase in the size of both burns as the lunar orbit inclination increases. Summing the two burns results in a total ΔV that ranges from 1.1526 km/s to 1.1581 km/s, a difference of 5.5 m/s. Figure 10 shows a parabolic behavior for the RAAN of the Earth orbit and an erratic behavior of true anomaly with increase in lunar inclination. It is important to note that while these plots show relationships between the optimization variable values and the choice of lunar orbit inclination, the overall change in the optimization values is not appreciable in most cases. This suggests that the lunar

orbit inclination does not have a large effect on the characteristics of the lunar transfer for inclinations within 50 deg of polar, when the transfer orbit is appropriately re-optimized using the Copernicus optimizer.

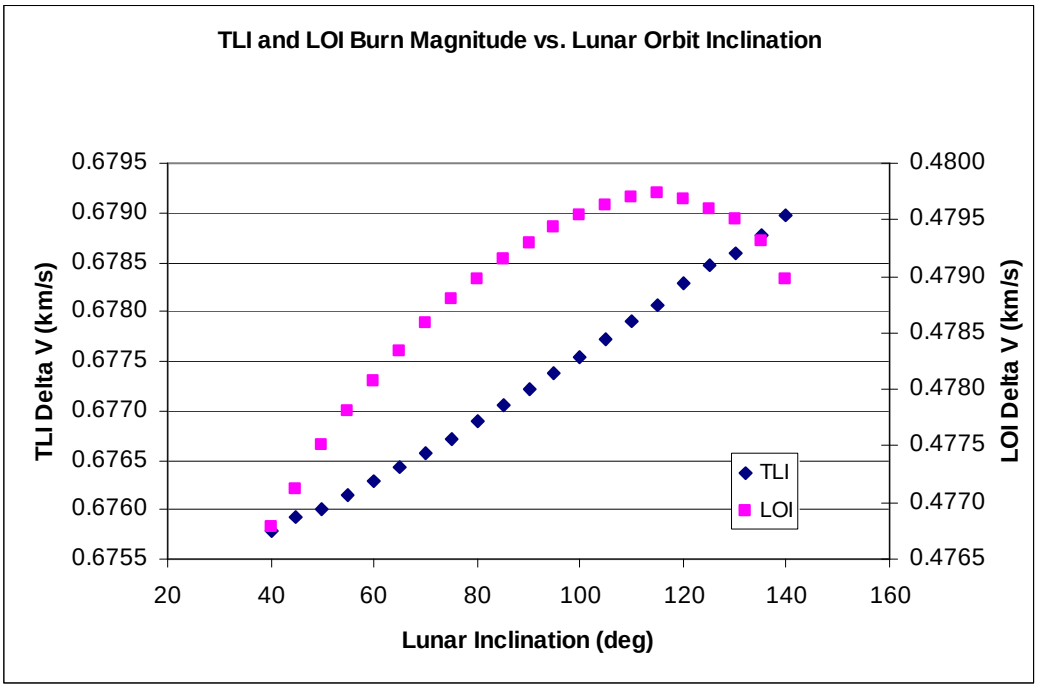

Figure 9

TLI and LOI Burn Magnitude vs. Lunar Orbit Inclination (18 deg inclination, 0 deg AoP GTO)

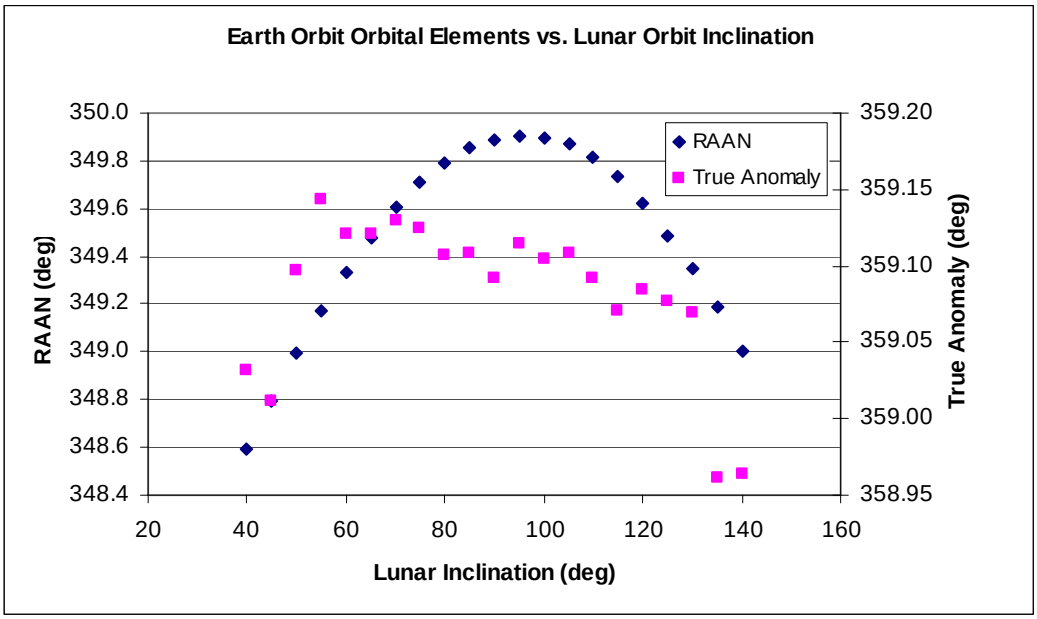

Figure 10

Earth Orbit Orbital Elements vs. Lunar Orbit Inclination (18 deg inclination, 0 deg AoP GTO)

Figures 11 and 12 show the change in final mass and LOI ΔV, respectively, as the AoP of the target lunar orbit is varied. Unlike the inclination variation plots, these plots show noticeable variation with change in AoP. As the AoP increases, the ΔV, and therefore the fuel mass requirement, decreases.

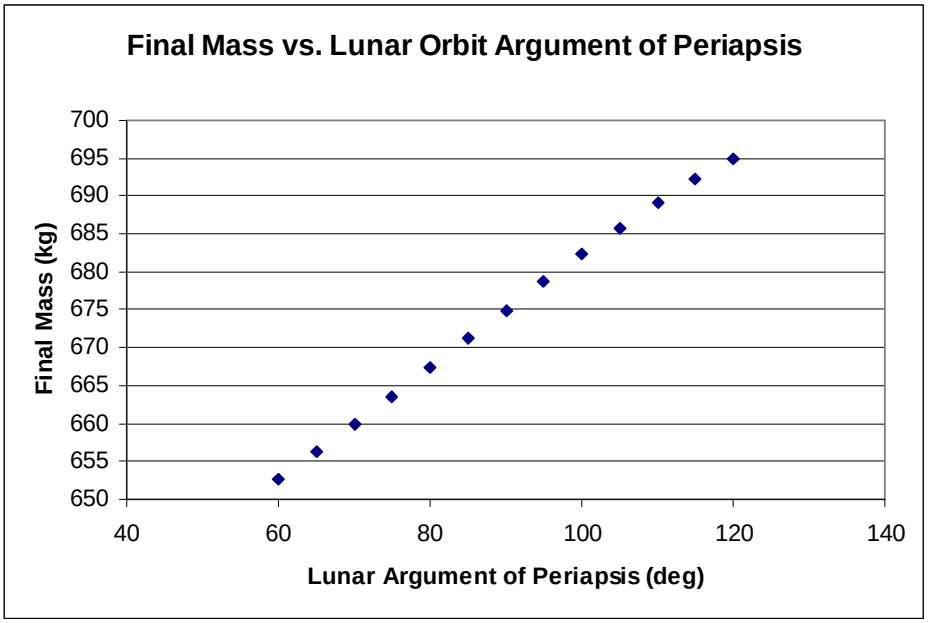

Figure 11

Final Spacecraft Mass vs. Lunar Orbit Argument of Periapsis (18 deg inclination, 0 deg AoP GTO)

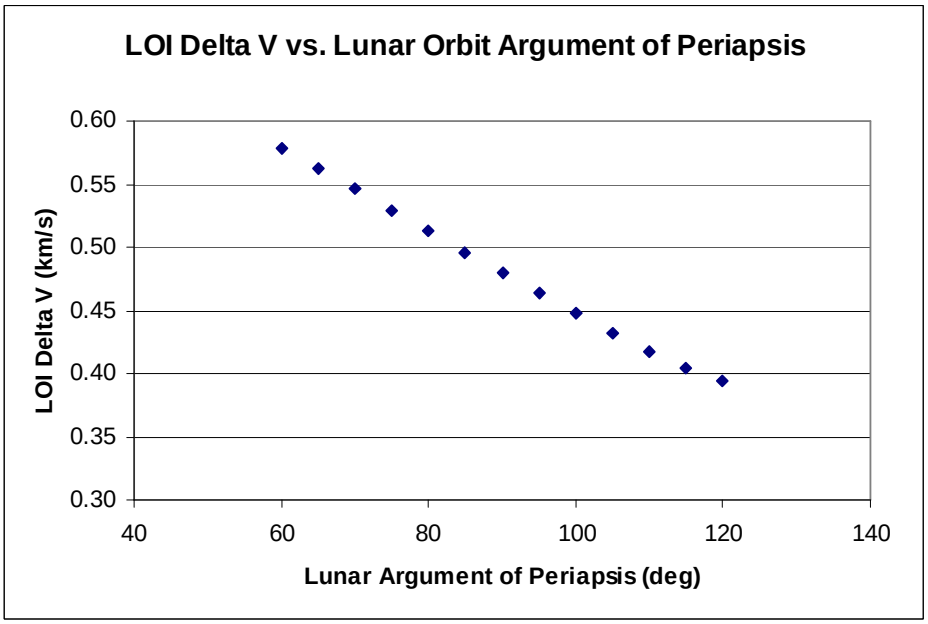

Figure 12

LOI Delta V vs. Lunar Orbit Argument of Periapsis (18 deg inclination, 0 deg AoP GTO)

Similar plots were created for the other Earth orbit AoP cases of the 18 deg inclination GTO Earth orbit. Some of the inclination variation plots follow the same behavior as the figures shown above, while others show different or no trends at all. The different trends suggest that similar lunar transfers can be achieved by varying the set of optimization variables in different ways. However, they all show the same small difference between the minimum and maximum values of the optimization variables. All of the plots resulting from the variation in lunar orbit AoP show the same, general behavior as Figures 11 and 12 though the exact minimum and maximum values change. Table 3 presents the average values for all optimization variables for each of the four initial Earth AoP cases for the lunar inclination variation optimizations. The average final mass variation is only 10.4 kg from the worst case to the best case explored. The transfer times are also similar with a maximum average difference of 8.64 hours between the four cases. Both cases where the AoP places the perigee of the Earth orbit at a node (0 deg and 180 deg) result in initial time deviations (from 12:00 GMT Jan 1 2012) of approximately 7.5 days. The off node perigees have initial times 4 days off from this time. The average TLI burn magnitude differs by 3.6 m/s, while the LOI magnitude varies by 48.8 m/s. The initial Earth orbit RAAN is clearly affected by the AoP of the Earth orbit, but the initial true anomaly for all cases is within one degree. These results show that viable trajectories are achievable for all four AoP cases over the full range of inclinations explored.

Table 3

Average Values for 18 deg Inclination Earth Orbit AoP Cases, Inclination Variation

0 deg AoP Earth Orbit	
Final Mass	675.05 kg
Transfer Time	4.78 days
Initial Time	7.45 days
Earth RAAN	349.48 deg
Earth True Anomaly	359.08 deg
TLI Magnitude	0.6773 km/s
LOI Magnitude	0.4788 km/s
Total Delta V	1.156 km/s
90 deg AoP Earth Orbit	
Final Mass	671.59 kg
Transfer Time	4.60 days
Initial Time	11.58 days
Earth RAAN	313.77 deg
Earth True Anomaly	0.28 deg
TLI Magnitude	0.6755 km/s
LOI Magnitude	0.4957 km/s
Total Delta V	1.171 km/s
180 deg AoP Earth Orbit	
Final Mass	677.31 kg
Transfer Time	4.80 days
Initial Time	7.36 days
Earth RAAN	168.43 deg
Earth True Anomaly	359.57 deg
TLI Magnitude	0.6774 km/s
LOI Magnitude	0.4689 km/s
Total Delta V	1.146 km/s
270 deg AoP Earth Orbit	
Final Mass	682.02 kg
Transfer Time	4.96 days
Initial Time	3.35 days
Earth RAAN	28.63 deg
Earth True Anomaly	359.94 deg
TLI Magnitude	0.6791 km/s
LOI Magnitude	0.4469 km/s
Total Delta V	1.126 km/s

90 Degree Inclination Earth Orbit

The 90 deg inclination Earth orbit optimizations followed the same process as that used for the 18 deg inclination cases. The same plots were created as for the 18 deg inclination case, and the plots show similar trends and very little difference in the minimum and maximum respective y-values for the inclination variation optimizations. The plots for the 90 deg Earth inclination, 0 deg Earth AoP case are shown in Figures 13-17. The final mass shows more variation with lunar orbit inclination than it did for the 18 deg Earth orbit inclination cases. This appears to be because the LOI ΔV also varies more than in the 18 deg inclination cases. The final mass variation remains relatively small though with a maximum difference of less than 5 kg.

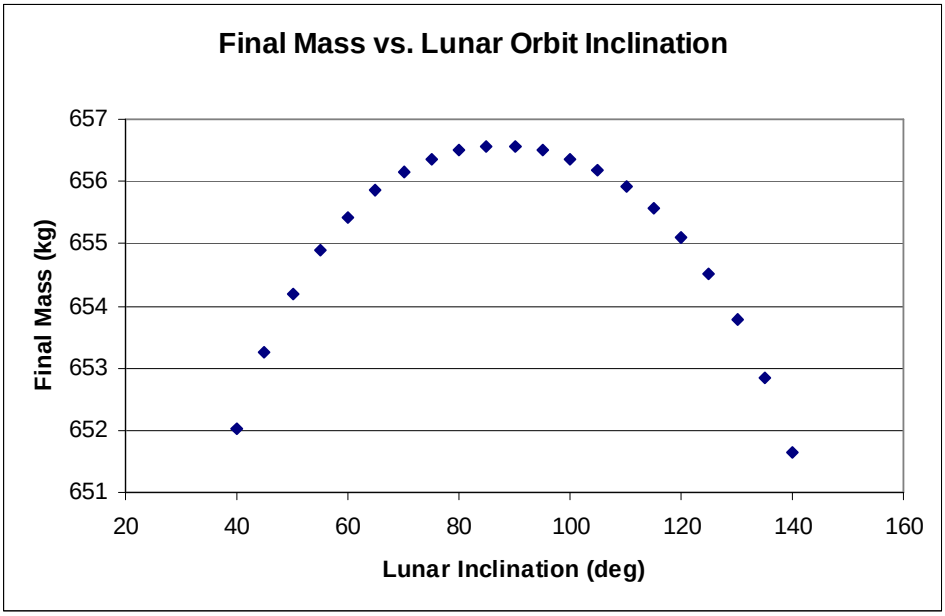

Figure 13

Final Spacecraft Mass vs. Lunar Orbit Inclination (90 deg inclination, 0 deg AoP GTO)

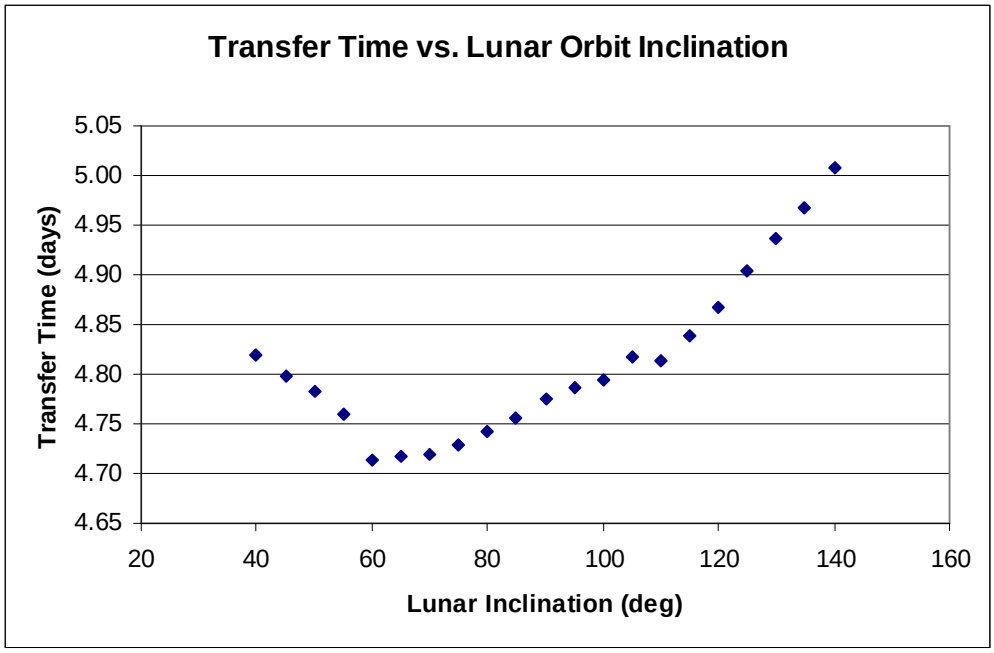

Figure 14

Transfer Time vs. Lunar Orbit Inclination (90 deg inclination, 0 deg AoP GTO)

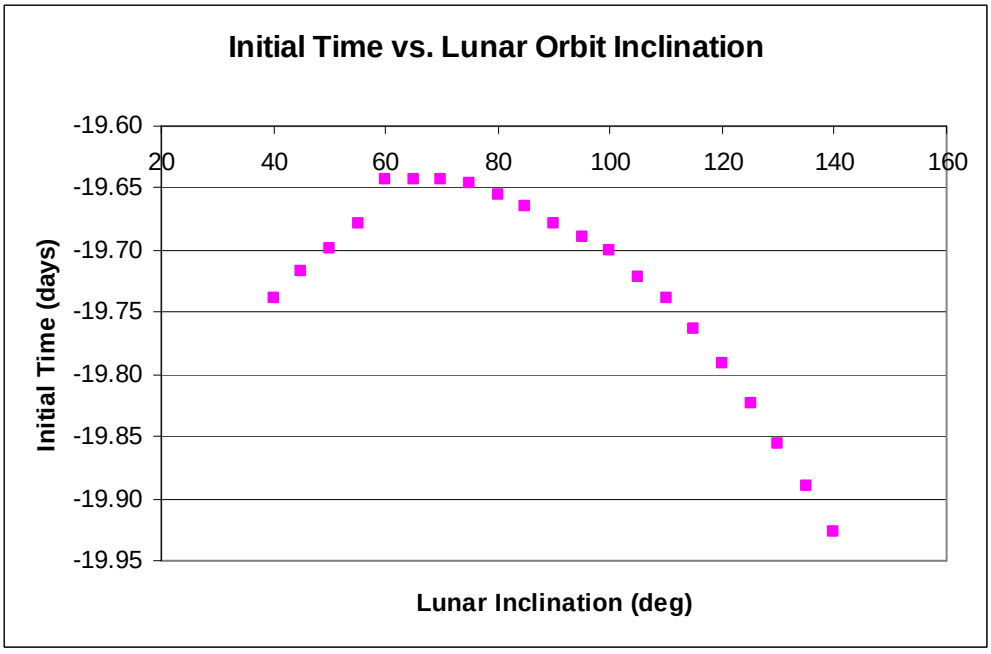

Figure 15

Initial Time vs. Lunar Orbit Inclination (90 deg inclination, 0 deg AoP GTO)

Figure 15 shows a large deviation in the initial time from the chosen epoch time for the scenario. The initial time deviated more than 19 days from the epoch, a considerable percentage of the orbital period of the Moon around the Earth. This deviation is necessary to get the proper launch date so that the alignment of the trajectory is correct. Because the LOI burn magnitude varies more than it did for the transfers using the 18 deg inclination initial Earth orbit, the total ΔV also varies more with a minimum value of 1.2378 km/s, for an 85 deg inclination lunar orbit, and a maximum value of 1.2600 km/s, for a 140 deg inclination lunar orbit. This is a total ΔV difference of 22.2 m/s.

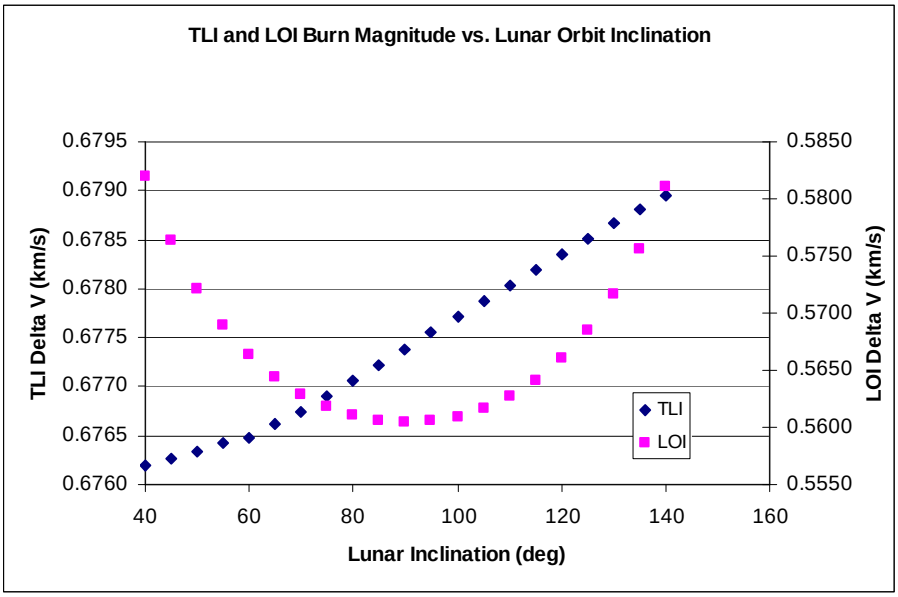

Figure 16

TLI and LOI Burn Magnitude vs. Lunar Orbit Inclination (90 deg inclination, 0 deg AoP GTO)

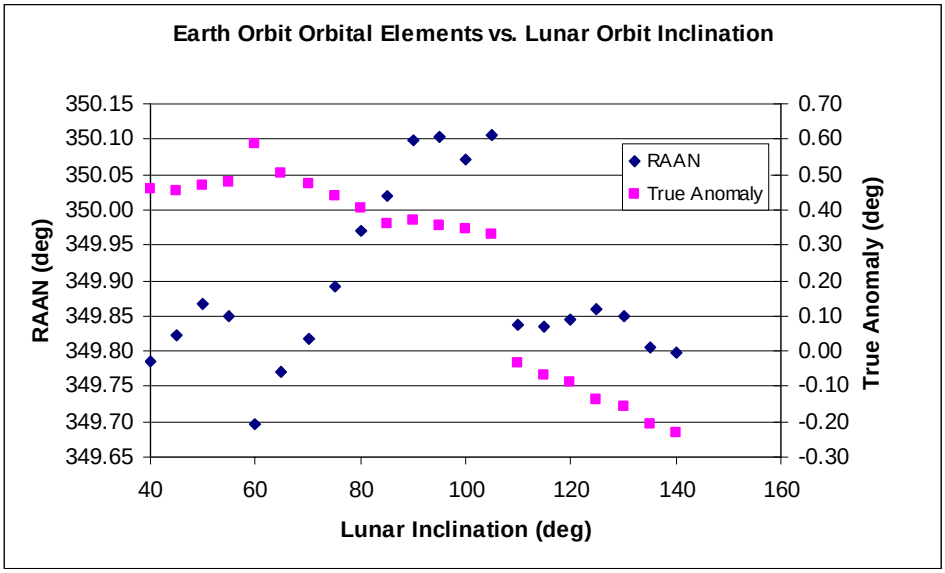

Figure 17

Earth Orbit Orbital Elements vs. Lunar Orbit Inclination (90 deg inclination, 0 deg AoP GTO)

Figures 18 and 19 are plots of the final mass and LOI ΔV requirement for the lunar orbit argument of periapsis variation for this same case. As with the 18 deg Earth orbit inclination cases, they show the same decrease in ΔV with increase in argument of periapsis.

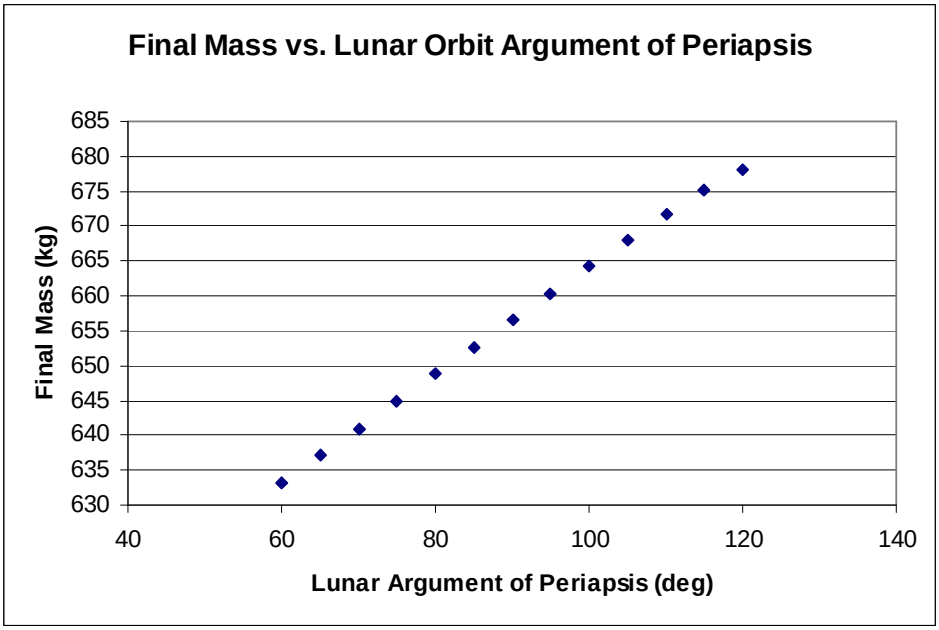

Figure 18

Final Spacecraft Mass vs. Lunar Orbit Argument of Periapsis (90 deg inclination, 0 deg AoP GTO)

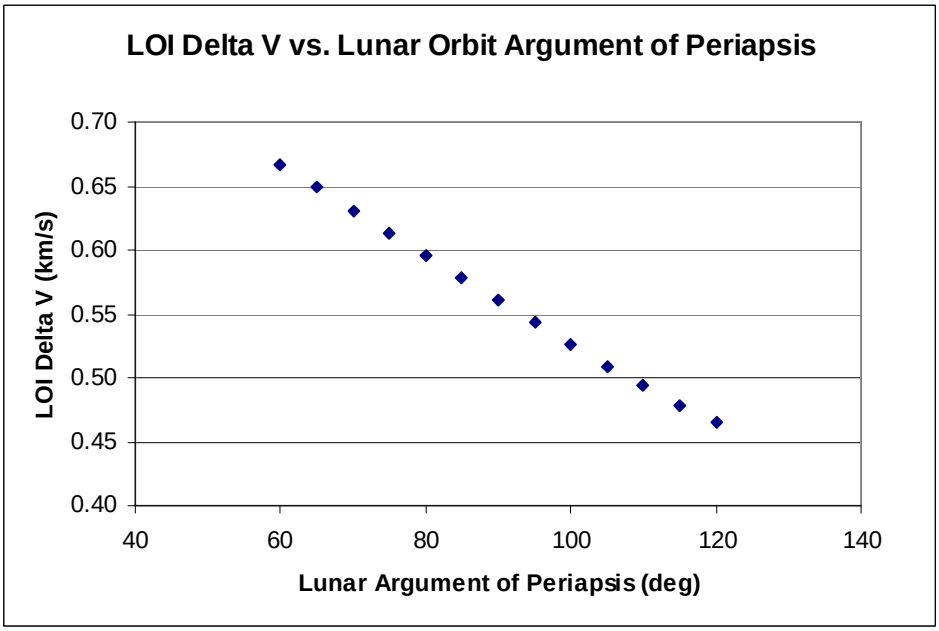

Figure 19

LOI Delta V vs. Lunar Orbit Argument of Periapsis (90 deg inclination, 0 deg AoP GTO)

The average of the optimization variables for the 90 deg Earth inclination GTO cases are presented in Table 4. The average final mass for both cases is within 5 kg. Since the orbit period of the Moon is approximately 28 days, the average initial times are comparable. The average transfer times differ by half a day. The average RAAN difference is approximately 180 degrees, which makes sense because the AoPs are separated by 180 degrees. The TLI burn average differs by 1.2 m/s, while the LOI burn difference is 19.1 m/s.

Table 4

Average Values for 90 deg Inclination Earth Orbit AoP Cases, Inclination Variation

0 deg AoP Earth Orbit	
Final Mass	655.06 kg
Transfer Time	4.81 days
Initial Time	-19.73 days
Earth RAAN	349.89 deg
Earth True Anomaly	0.24 deg
TLI Magnitude	0.6774 km/s
LOI Magnitude	0.5671 km/s
Total Delta V	1.244 km/s
180 deg AoP Earth Orbit	
Final Mass	659.06 kg
Transfer Time	5.31 days
Initial Time	6.63 days
Earth RAAN	165.05 deg
Earth True Anomaly	1.52 deg
TLI Magnitude	0.6786 km/s
LOI Magnitude	0.5480 km/s
Total Delta V	1.227 km/s

Finally, Table 5 compares the total ΔVs and final masses for the 18 and 90 deg Earth orbit inclination cases. All of the 18 deg inclination cases result in higher final masses and, equivalently, lower total ΔVs than the 90 deg inclination cases. The final

mass difference between the most fuel optimal 18 deg inclination case, 270 deg Earth AoP, and the most fuel optimal 90 deg inclination case, 180 deg Earth AoP, is 23 kg.

Table 5

Summary of Impulsive Burn Cases

18 deg Earth Inclination	
0 deg Earth AoP	
Final Mass	675.05 kg
Total Delta V	1.156 km/s
90 deg Earth AoP	
Final Mass	671.59 kg
Total Delta V	1.171 km/s
180 deg Earth AoP	
Final Mass	677.31 kg
Total Delta V	1.146 km/s
270 deg Earth AoP	
Final Mass	682.02 kg
Total Delta V	1.126 km/s

90 deg Earth Inclination	
0 deg Earth AoP	
Final Mass	655.06 kg
Total Delta V	1.244 km/s
180 deg Earth AoP	
Final Mass	659.06 kg
Total Delta V	1.227 km/s

Sources: [1]International Reference Guide to Space Launch Systems, [2]MagnoliaRequirements_Nov2007.xls, [3]Mechanics and Thermodynamics of Propulsion, p. 473.

CHAPTER IV

FINITE BURN TRANSFERS

Like the impulsive burn optimizations, finite burn transfer optimizations were completed using both 18 deg and 90 deg inclination initial Earth orbits. The 18 deg inclination runs were completed first and the 90 deg runs were completed after further clarification from SSTL on the current baseline mission design for the proposed lunar small satellite mission. A staged process similar to that used for the impulsive burn optimizations was employed to optimize the finite burn transfers.

The first step was to optimize the TLI burn. To do this, the finite burn engine was activated in Copernicus and the propulsion system was defined. In this case, the system was defined by specifying the thrust and specific impulse. All finite burn transfers discussed in this chapter were done assuming a thrust of 100 N and an I_{sp} of 300 s as provide by SSTL. Then the sub-optimal control parameters were assigned initial values. The direction of thrust was parameterized using α, the angle of thrust in the orbit plane with respect to the orbital velocity vector, and its first two derivatives, $\dot{\alpha}$ and $\ddot{\alpha}$. However, test runs showed that inclusion of the second derivative did not contribute significantly to the optimization results. The resulting $\ddot{\alpha}$ values were nearly zero, and since both $\dot{\alpha}$ and $\ddot{\alpha}$ are defined in Copernicus with units of deg/day, small $\ddot{\alpha}$ values would not have a significant effect over the course of burns of duration of one to two hours. So $\ddot{\alpha}$ was disabled to simplify the optimization procedure. For the TLI, the initial values for

α and $\dot{\alpha}$ were set to zero, meaning the thrust would always be in the direction of the velocity vector.

Since finite burns are applied over an entire segment in Copernicus, an initial estimate of the length of the burn is input by changing the DT of the segment. The burn time for such a low thrust engine can be expected to be on the order of several hours, according to preliminary results from SSTL, so a good initial guess is two to three hours. Finally a coast segment must be connected to the burn segment to allow the spacecraft to rendezvous with the Moon. Using the results of the impulsive burn optimizations, a coast period of approximately five days was used as an initial estimate. This estimate could also be further improved by using the Copernicus visualization options to choose a coast period that roughly intercepts the Moon. The target condition for the TLI optimization was an orbit radius vector of zero magnitude with respect to the Moon. In other words, at this step, the Moon itself is the target.

After the TLI burn was optimized, the next step was to align the spacecraft for lunar orbit insertion. As with the impulsive burn optimizations, a frozen orbit was used as the target lunar orbit. The orbit listed in Table 6 was used for the 18 deg inclination optimizations, and a modified version was used for the 90 deg inclination optimization runs. The alignment process for lunar orbit insertion was the same as used for the impulsive burn cases. The Moon's gravity was enabled, and the inclination and argument of periapsis of the lunar orbit were set as targets. Maximum and minimum radius magnitude constraints were also set, and the radial velocity at the end of the coast segment was constrained to be zero.

Table 6

Lunar Frozen Orbit (Ely)[11]

Semi-major Axis	6541.4 km
Eccentricity	0.6
Inclination	63.01 deg
Right Ascension of the Ascending Node	0 deg
Argument of Periapsis	90 deg

Once proper alignment was achieved, the LOI burn was then optimized. For the LOI burn, the initial thrust direction was assumed to be in the anti-velocity direction with an $\dot{\alpha}$ of zero. As with the TLI burn, inclusion of the second derivative, $\ddot{\alpha}$, was found to be unnecessary.

18 Degree Inclination Earth Orbit

TLI burn optimizations were done over the complete range of initial Earth orbit argument of perigee values. The argument of perigee was changed in 5 deg increments from 0 to 360 deg. Figures 20, 21, and 22 were created from the results.

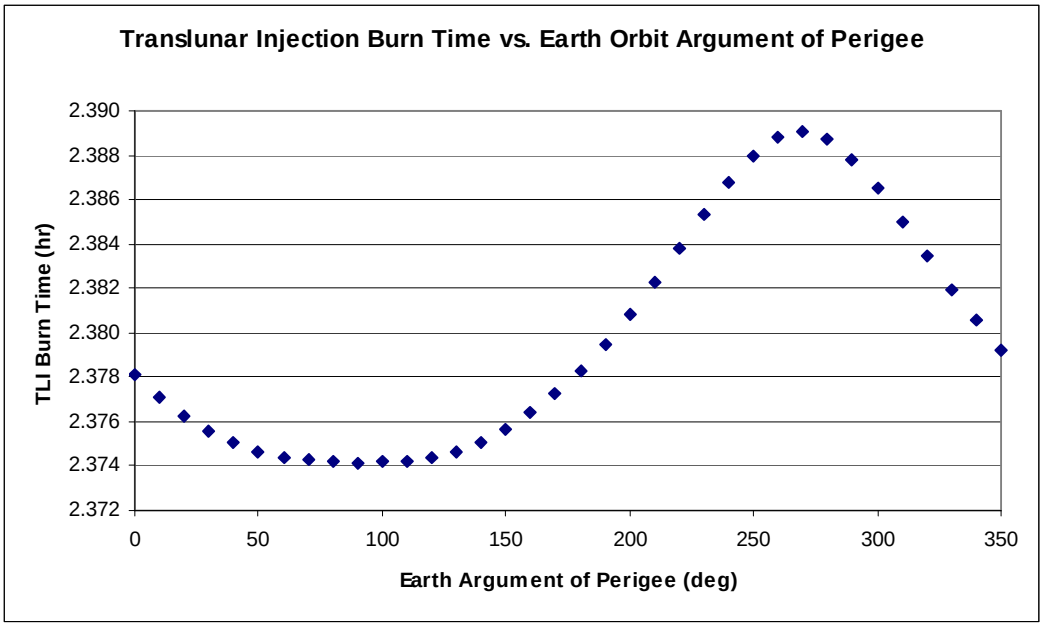

Figure 20

TLI Burn Time vs. Earth Orbit Argument of Perigee (18 deg inclination GTO)

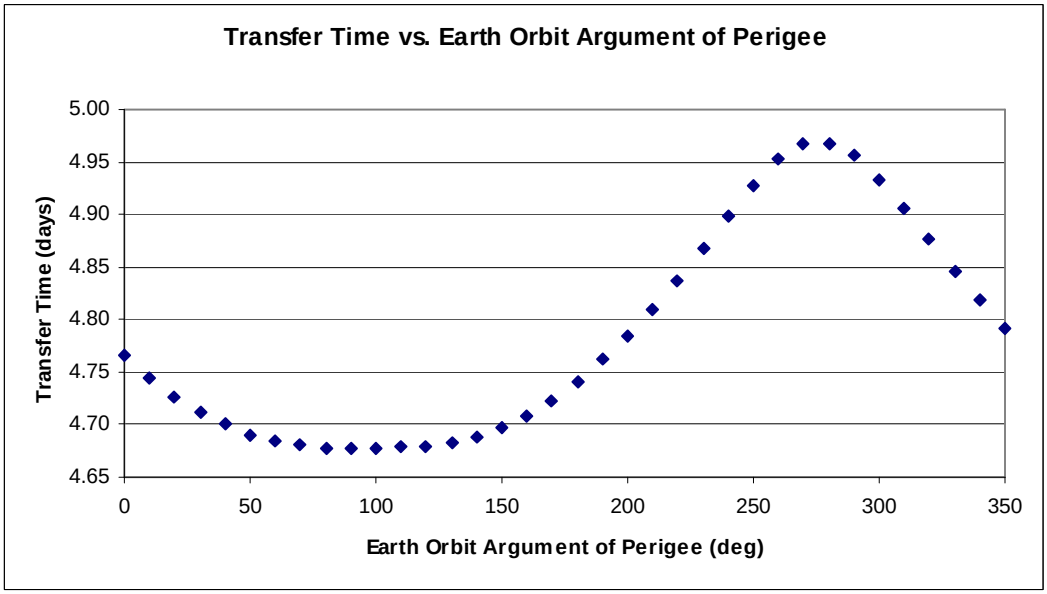

Figure 21

Transfer Time vs. Earth Orbit Argument of Perigee (18 deg inclination GTO)

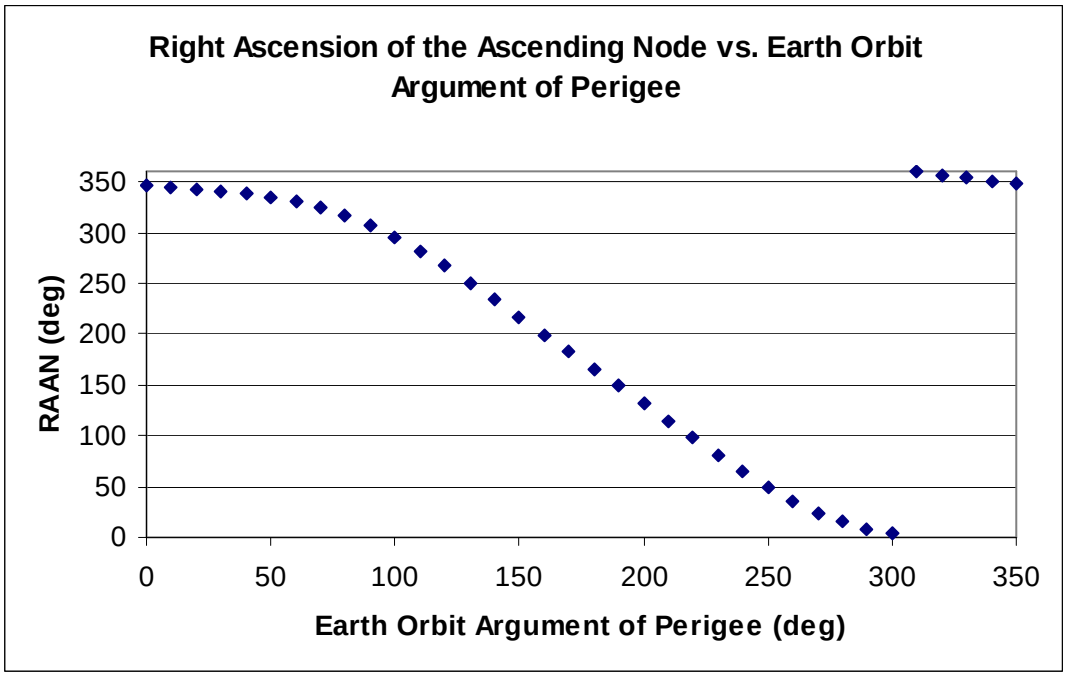

Figure 22

RAAN vs. Earth Orbit Argument of Perigee (18 deg inclination GTO)

Figures 20 and 21 show almost identical sinusoidal or oscillating patterns. The TLI burn time is at a minimum when the argument of perigee of the Earth orbit is approximately 90 deg and a maximum near an AoP of 270 deg, and the transfer time has extrema at similar AoP values. Although there is a discernible pattern, there is not a significant difference between the minimum and maximum values of the burn time, meaning the ΔVs are similar, but the transfer time varies by approximately 7 hours. In Figure 22, the RAAN is zero for an AoP of 300 deg and increases as the argument of perigee decreases and then repeats.

Next complete transfer optimizations were done over a range of lunar inclinations for initial Earth orbits with AoPs of 0, 90, 180, and 270 deg. Variables that determine the alignment of the lunar transfer, such as the initial time and Earth orbit RAAN, were very

similar to the corresponding impulsive burn cases. The variables of interest to compare the impulsive and finite burn cases are the burn times for both the TLI and LOI maneuvers as well as the final mass. Table 7 summarizes the average values of these variables for the four AoP cases. As burn time increases, the fuel mass required increases. Therefore, shorter burn times will result in a more fuel optimal transfer and a greater final mass. So the most fuel optimal transfer will have the shortest total burn time and the highest final mass.

Table 7

Average Values for 18 deg Inclination Earth Orbit AoP Cases, Inclination Variation

0 deg AoP Earth Orbit	
Final Mass	608.37 kg
TLI Burn Time	2.38 hrs
LOI Burn Time	0.82 hrs
90 deg AoP Earth Orbit	
Final Mass	606.25 kg
TLI Burn Time	2.37 hrs
LOI Burn Time	0.84 hrs
180 deg AoP Earth Orbit	
Final Mass	605.88 kg
TLI Burn Time	2.41 hrs
LOI Burn Time	0.81 hrs
270 deg AoP Earth Orbit	
Final Mass	612.55 kg
TLI Burn Time	2.39 hrs
LOI Burn Time	0.77 hrs

Like the impulsive burn cases, there is not much difference in the propulsive requirement for the different AoP cases of the Earth orbit. Table 8 shows the final mass difference between the analogous impulsive and finite burn cases for the 18 deg inclination initial Earth GTO. The finite burn cases require more fuel than the impulsive

burn cases. The difference is significant reinforcing the assumption that the burns should not be modeled as impulsive.

Table 8

Impulsive vs. Finite Burn Final Mass Difference (18 deg inclination GTO)

Earth Argument of Perigee (deg)	Final Mass Difference (kg)
0	66.62
90	65.56
180	70.78
270	68.74

90 Degree Inclination Earth Orbit

Like the 18 deg inclination Earth orbit case, TLI burn optimizations were completed with the 90 deg inclination Earth GTO for a range of argument of perigee values. However, since AoPs near 90 and 270 deg are not realistic candidates because of the unfavorable alignment of the GTO's line of apsides, only AoPs around 0 and 180 deg were explored. This fact would have important implications for the deisng of the Earth orbit and launch window of the mission. The results for AoPs centered around 0 deg are shown in Figures 23, 24, and 25 and similarly in Figures 26, 27, and 28 for AoPs centered around 180 deg.

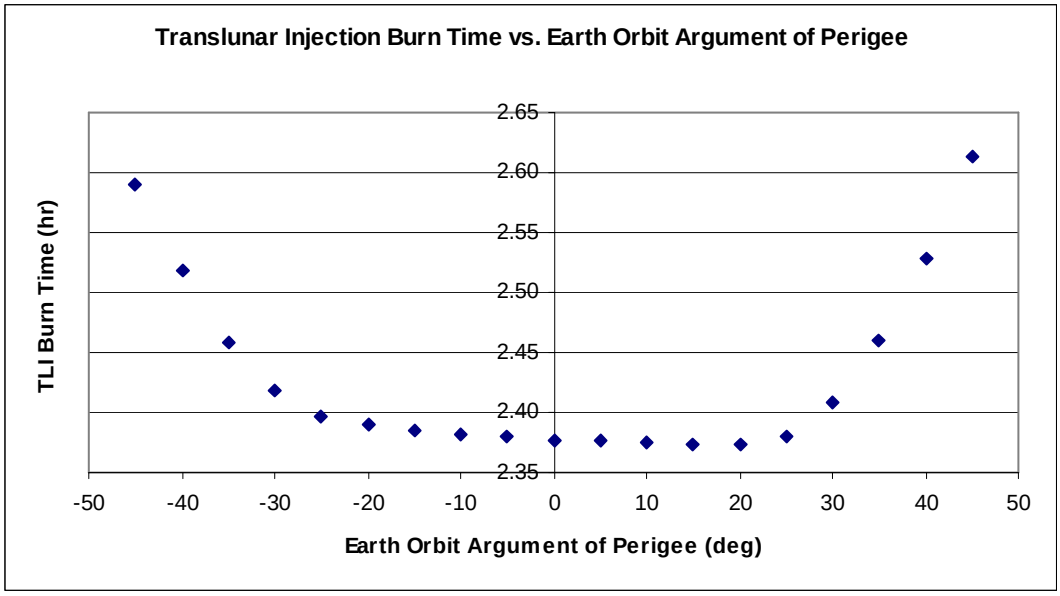

Figure 23

TLI Burn Time vs. Earth Orbit Argument of Perigee (90 deg inclination GTO, 0 deg AoP range)

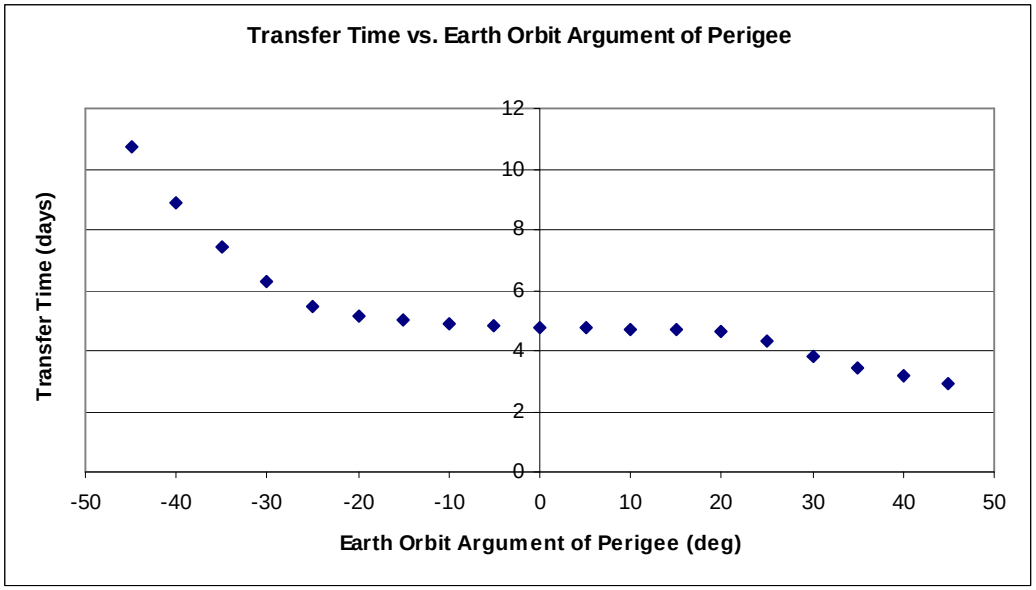

Figure 24

Transfer Time vs. Earth Orbit Argument of Perigee (90 deg inclination GTO, 0 deg AoP range)

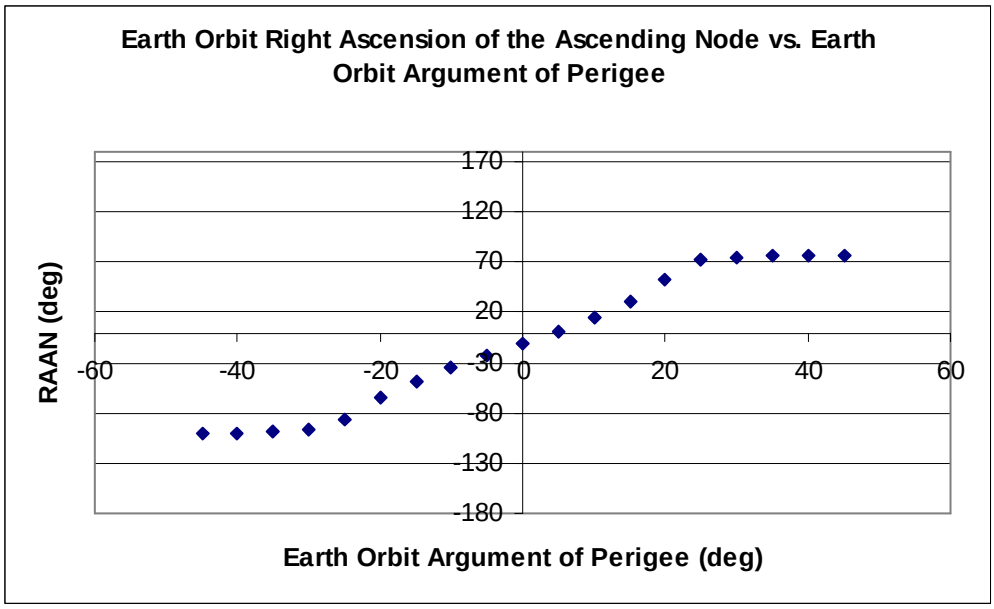

Figure 25

RAAN vs. Earth Orbit Argument of Perigee (90 deg inclination GTO, 0 deg AoP range)

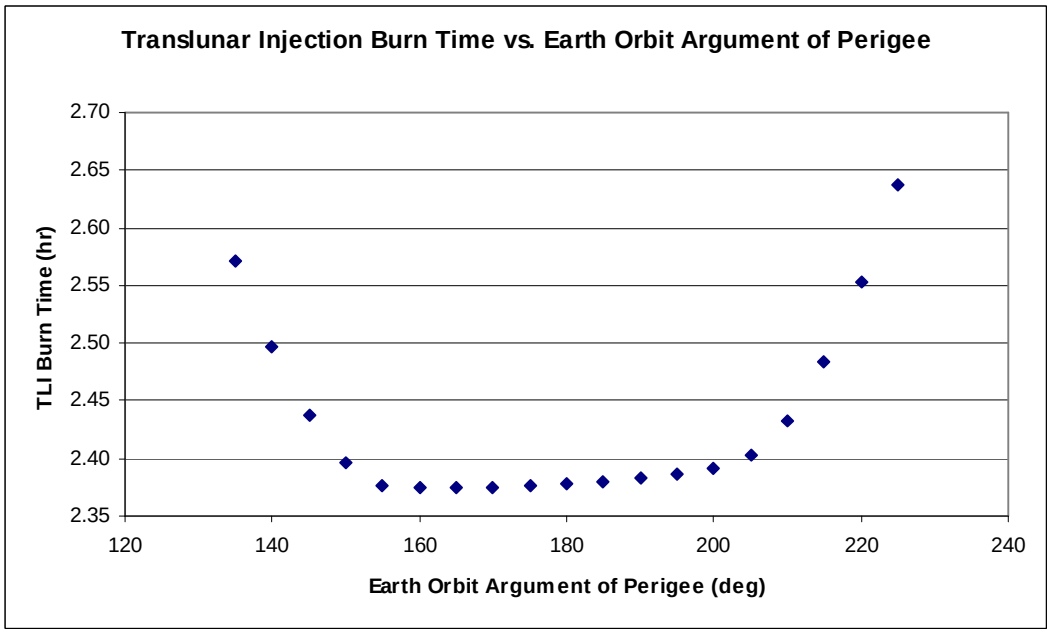

Figure 26

TLI Burn Time vs. Earth Orbit Argument of Perigee (90 deg inclination GTO, 180 deg AoP range)

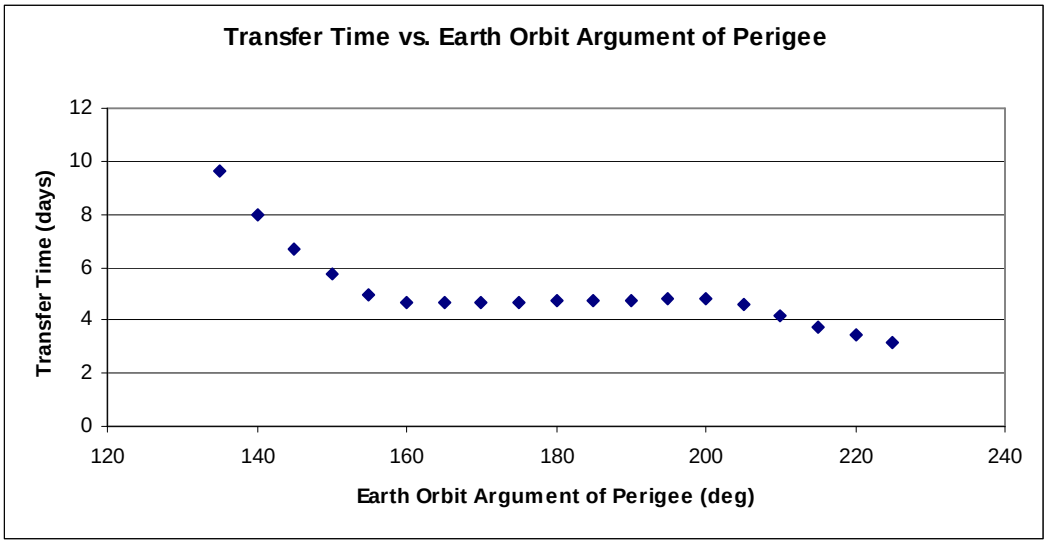

Figure 27

Transfer time vs. Earth Orbit Argument of Perigee (90 deg inclination GTO, 180 deg AoP range)

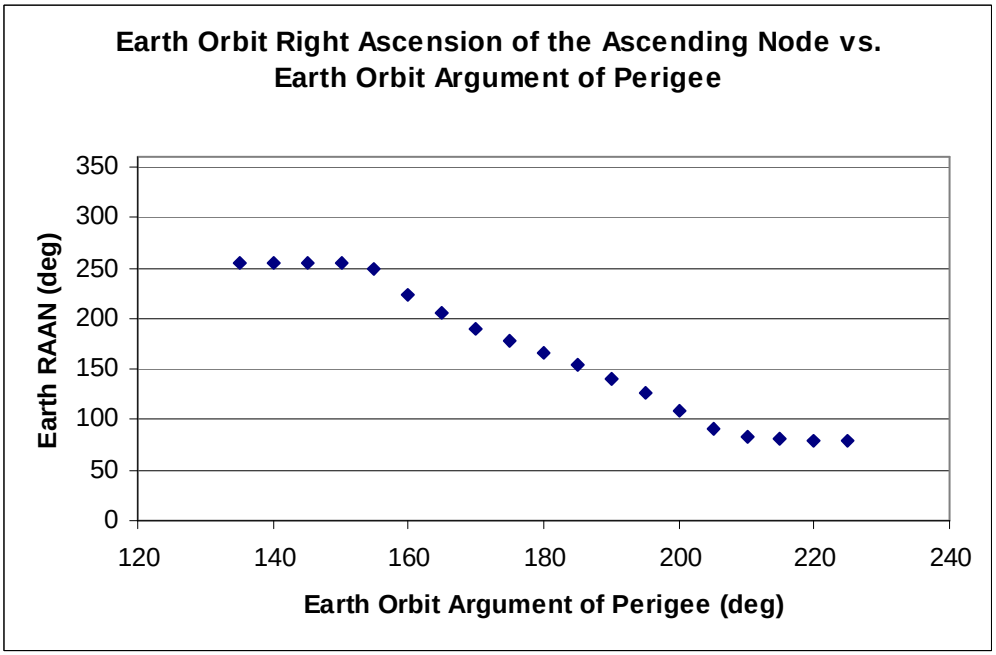

Figure 28

RAAN vs. Earth Orbit Argument of Perigee (90 deg inclination GTO, 180 deg AoP range)

Unlike the 18 deg inclination cases, there are significant correlations between the argument of perigee and the burn time, transfer time, and RAAN. Because of the comparatively low inclination of the 18 deg orbit, changing the AoP did not significant change the required declination of the Moon for lunar intercept, so all transfers could intersect the Moon near its orbit's descending node.

However, for the 90 deg inclination Earth orbit, as the AoP moves away from 0 or 180 deg, the point at which the transfer orbit intersects the Moon moves away from the Moon's orbit's node. This results in first a gradual change in both the burn time and transfer time for AoPs near 0 or 180 deg, but as the AoP gets farther away, these variables change dramatically because the transfer orbit is no longer intersecting the Moon when the spacecraft is at the apogee of the transfer orbit with respect to the Earth. Once the AoP of the Earth orbit is such that the required lunar declination is greater than the inclination of the Moon's orbit, the spacecraft must be placed in a transfer orbit with an apogee radius greater than the radius of the Moon's orbit, which is an inherently more inefficient transfer. This behavior is demonstrated in Figures 29 and 30. In Figure 29, the lunar transfer reaches the Moon near the apogee point of the transfer orbit. While in Figure 30, the apogee point is now beyond the Moon's orbit.

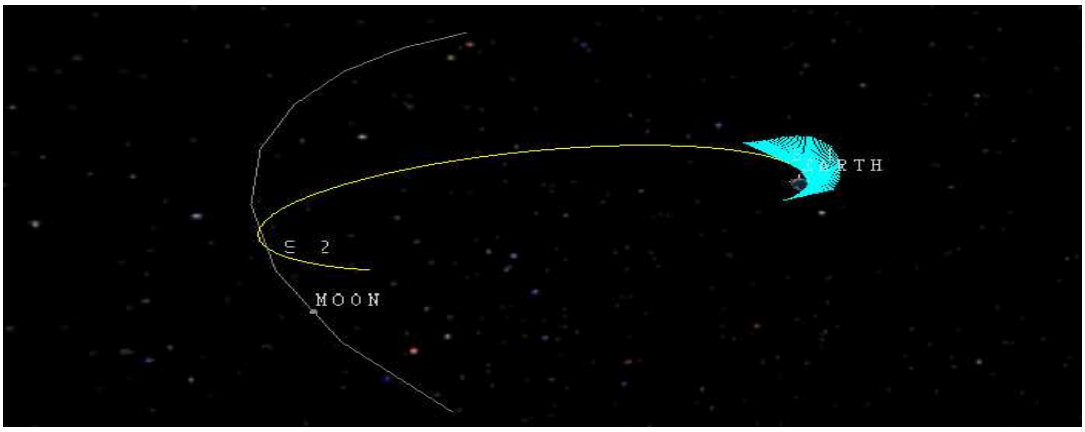

Figure 29

Lunar Transfer Orbit Example (lunar intercept at apogee)

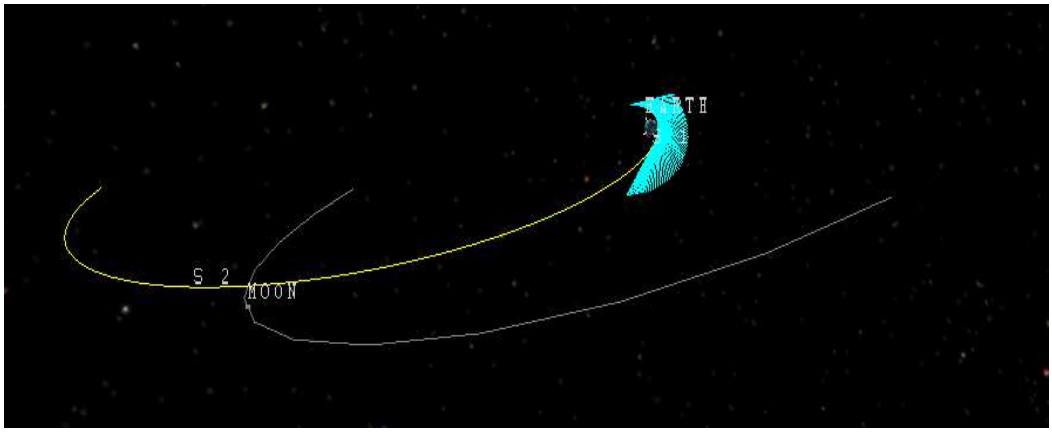

Figure 30

Lunar Transfer Orbit Example (lunar intercept before apogee)

For each AoP range, three AoPs were chosen for optimization of complete lunar transfers. The AoP with the lowest burn time as well as the two endpoints of each AoP range were selected. For the 0 deg AoP range, this corresponded to AoPs of -45, 20, and 45 deg, and for the 180 deg range, AoPs of 135, 160, and 225 deg were chosen. Table 9 summarizes the results of these optimizations. Comparing these results to those in Table 7, transfers using a 90 deg inclination Earth orbit appear to be less fuel optimal. Except

for the 225 AoP case, the LOI burn times for the 90 deg Earth orbit inclination cases are all noticeably longer than the 18 deg Earth orbit inclination cases, and the TLI burn times are also longer except for the AoP cases near 0 and 180 deg. This is likely because most of these transfers intercept the Moon away from the descending node of its orbit.

Table 9

90 deg Inclination Transfer Results

Argument of Perigee (deg)	TLI Burn Time (hr)	Transfer Time (days)	LOI Burn Time (hr)	Total Burn Time (hr)	Final Mass (kg)
-45	2.58	10.90	1.08	3.66	551.58
20	2.37	4.42	1.11	3.48	573.90
45	2.67	3.54	1.10	3.77	538.84
135	2.64	8.32	1.08	3.72	544.96
160	2.37	4.56	1.03	3.41	583.97
225	2.68	4.03	0.85	3.53	567.44

One additional finite burn transfer optimization was completed on a new mission baseline orbit provided by SSTL late in the course of this study. The initial Earth orbit was also refined with the argument of perigee specified to be 178.5 deg and the shape slightly modified. The parameters of the new mission orbit and the initial Earth orbit are provided in Tables 10 and 11. The results of the optimization are given in Table 12. Comparing these results to the other 90 deg inclination Earth orbit finite burn optimizations shows that this transfer results in the greatest final mass of the 90 deg Earth inclination cases studied.

Table 10

New Baseline Lunar Orbit

Periapsis Radius	2454 km
Apoapsis Radius	9826 km
Inclination	57.7 deg
Argument of Periapsis	90 deg

Table 11

Modified GTO Earth Orbit

Semi-major Axis	24478.1 km
Eccentricity	0.731
Inclination	90 deg
Argument of Perigee	178.5 deg

Table 12

Transfer Optimization Results for New Mission Orbit

TLI Burn Time (hr)	**Transfer Time (days)**	**LOI Burn Time (hr)**	**Final Mass (kg)**
2.37	4.78	1.01	587.00

CHAPTER V

PHASED TRANSFERS

Phased transfers were explored to determine the possible fuel savings that could be achieved if gravity losses were decreased by performing several smaller burns at perigee of the Earth orbit instead of one single larger TLI burn. As an initial estimate, phased transfers were completed to raise the apogee of the GTO orbit to that of the semi-major axis of the Moon's orbit, 384,000 km. Four different phased burn sequences were explored. These were 50-75-100-200-384, 50-100-200-384, 75-150-384, and 100-200-300-384, where each number is the new apogee radius in thousands of kilometers after a burn. These transfers require five, four, three, and four burns respectively.

These sequences were chosen to explore how the fuel requirement is affected by when and how much the apogee radius is increased in one burn. The first sequence increases the apogee gradually at first until the apogee radius has increased significantly. At which point, the apogee is increased in larger increments. Each of the next three sequences increases the apogee radius more quickly. Although attempts were made to use Copernicus to optimize how much each burn should increase the apogee radius, because of the complexity of the search space, repeated burns separated by coast periods, the initial attempts were not successful. The author decided to manually choose a variety of sequences to explore the phased transfer behavior. The modified baseline mission

orbit and initial Earth GTO given in Tables 10 and 11 at the end of Chapter IV were used for the phased transfer optimizations.

The optimization results from the four phased transfer cases are presented in Table 13. One characteristic that is obvious from these results is that the required burn duration to further raise the apogee of the transfer decreases as the apogee point gets farther from the Earth. The first case where the initial apogee raising is done in 25,000 km increments results in the highest final mass, while the third case, where each of the first two burns raises the apogee by 100,000 km, shows the worst performance. For comparison, a single burn transfer from the GTO in Table 12 to an apogee radius of 384,000 km results in a burn time of 2.37 hr, a transfer time of 4.95 days, and a final mass of 709 kg. The fourth case is the second most fuel optimal, but it has the additional benefit of a total transfer time that is more than three days shorter than the most fuel optimal case.

Table 13

Phased Transfer TLI Results (100 N Thrust)

50-75-100-200-384 Phased Transfer							
Burn 1 Duration (hr)	Burn 2 Duration (hr)	Burn 3 Duration (hr)	Burn 4 Duration (hr)	Final Burn Duration (hr)	Total Burn Time (hr)	Total Transfer Time (days)	Final Mass (kg)
0.299	0.528	0.267	0.415	0.183	1.692	11.75	786

50-100-200-384 Phased Transfer						
Burn 1 Duration (hr)	Burn 2 Duration (hr)	Burn 3 Duration (hr)	Final Burn Duration (hr)	Total Burn Time (hr)	Total Transfer Time (days)	Final Mass (kg)
0.299	0.95	0.455	0.191	1.895	10.69	768

100-200-300-384 Phased Transfer						
Burn 1 Duration (hr)	Burn 2 Duration (hr)	Burn 3 Duration (hr)	Final Burn Duration (hr)	Total Burn Time (hr)	Total Transfer Time (days)	Final Mass (kg)
1.6	0.386	0.114	0.050	2.150	17.00	737

75-150-384 Phased Transfer					
Burn 1 Duration (hr)	Burn 2 Duration (hr)	Final Burn Duration (hr)	Total Burn Time (hr)	Total Transfer Time (days)	Final Mass (kg)
0.969	0.566	0.324	1.859	8.57	773

At this stage, the effect of the thrust level of the propulsion system was explored by running the same sequence of phased transfers with a 150 N thrust engine instead of the 100 N thrust engine used for all of the previous optimizations. The results from the 150 N phased transfers are shown below in Table 14. The 150 N thrust cases show improved performance over the 100 N cases for each transfer. However, there is less difference between the final masses for the 150 N cases. Using a single burn transfer

would result in a burn time of 1.39 hr, a transfer time of 4.98 days, and a final mass of 744 kg.

Table 14

Phased Transfer TLI Results (150 N Thrust)

50-75-100-200-384 Phased Transfer							
Burn 1 Duration (hr)	Burn 2 Duration (hr)	Burn 3 Duration (hr)	Burn 4 Duration (hr)	Final Burn Duration (hr)	Total Burn Time (hr)	Total Transfer Time (days)	Final Mass (kg)
0.196	0.375	0.174	0.27	0.121	1.136	11.65	791

50-100-200-384 Phased Transfer						
Burn 1 Duration (hr)	Burn 2 Duration (hr)	Burn 3 Duration (hr)	Final Burn Duration (hr)	Total Burn Time (hr)	Total Transfer Time (days)	Final Mass (kg)
0.196	0.582	0.266	0.121	1.165	10.70	786

100-200-300-384 Phased Transfer						
Burn 1 Duration (hr)	Burn 2 Duration (hr)	Burn 3 Duration (hr)	Final Burn Duration (hr)	Total Burn Time (hr)	Total Transfer Time (days)	Final Mass (kg)
0.828	0.266	0.083	0.037	1.214	16.93	777

75-150-384 Phased Transfer					
Burn 1 Duration (hr)	Burn 2 Duration (hr)	Final Burn Duration (hr)	Total Burn Time (hr)	Total Transfer Time (days)	Final Mass (kg)
0.598	0.364	0.212	1.174	8.48	784

Finally complete phased transfer optimizations were done by taking several of the phased transfer cases and applying LOI burns. The results of these optimizations are shown below for the 100 N and 150 N thrust cases in Tables 15 and 16 respectively. The first two transfers for each thrust level result in nearly identical final masses, while the third transfer has a higher fuel mass requirement for both thrust levels. Compared to the

single TLI burn case results shown in Table 12 using a 100 N thrust engine, the phased transfer requires from 22 to 51 kg less fuel. A single TLI burn transfer was also done with a 150 N thrust engine, and it resulted in a final mass of 616 kg, or 25 to 35 kg less than the equivalent phased transfers.

Table 15

Complete Phased Transfer Results (100 N Thrust)

Transfer Type	Total Transfer Time (days)	LOI Burn Time (hr)	Final Mass (kg)
50-100-Moon	6.59	1.10	636
75-150-Moon	8.43	1.11	638
100-200-Moon	10.32	1.05	609

Table 16

Complete Phased Transfer Results (150 N Thrust)

Transfer Type	Total Transfer Time (days)	LOI Burn Time (hr)	Final Mass (kg)
50-100-Moon	6.65	0.725	651
75-150-Moon	8.30	0.732	651
100-200-Moon	10.05	0.746	641

CHAPTER VI

SUMMARY AND CONCLUSIONS

This study began with analysis and optimization of direct impulsive burn transfers from an Earth-centered geostationary transfer orbit to a specified lunar "frozen" orbit. Two different inclination initial Earth orbits, 18 and 90 deg, were analyzed to see the effect on the total change in velocity required to complete the lunar transfer. For each of the two inclination orbits, the argument of perigee was also varied to see if this affected the propulsion requirements. For the 18 deg inclination Earth orbit, arguments of perigee explored were 0, 90, 180, and 270 deg. Because an argument of perigee of 90 or 270 degs would create an unfavorable alignment of the line of apsides for the 90 deg inclination Earth orbit, only arguments of perigee of 0 and 180 deg were explored for that case.

For each of the six total initial Earth orbit cases, transfers were completed and optimized to a given lunar frozen orbit. The inclination of this lunar orbit was varied from 40 to 140 deg to see if this affected the transfer requirements. The results showed that the inclination of the lunar orbit, in this extended polar range, has a minimal effect on the fuel requirements of individual, optimized transfers. Because there were many optimization variables that could be altered to complete the transfer, plots of the variation of these optimization variables with respect to lunar inclination showed different trends for the different Earth orbit cases. This suggests that suitable transfers can be achieved

by varying the optimization variables in different ways. The optimizations that started from an 18 deg inclination Earth orbit resulted in more fuel optimal transfers for the specific target orbit used. The average final mass for the 18 deg inclination cases was 676 kg, and the average final mass for the 90 deg inclination cases was 657 kg, assuming an initial mass of 1000 kg.

The lack of major differences between the various initial Earth orbit argument of perigee and lunar orbit inclination cases is evidence of the usefulness of the Copernicus software. The software was able to find similar optimal solutions for all of the cases. Excluded from this are the 90 and 270 deg Earth orbit argument of perigee cases for the 90 deg inclination initial Earth GTO. Because of the inherent geometry of these orbits, no comparable fuel optimal solutions are possible.

Using a 90 deg inclination lunar orbit, the argument of periapsis of the lunar orbit was also varied, from 60 to 120 deg, to find its effect on the ΔV required to complete the transfer. Unlike the inclination of the lunar orbit, the argument of periapsis of the lunar orbit did show a significant effect on the transfer requirements for both the 18 and 90 deg inclination initial Earth orbits. Both in-plane components of the lunar orbit insertion ΔV decreased with increasing argument of periapsis. The final mass after all maneuvers were completed was 40-50 kg greater for an argument of periapsis of 120 deg compared to an argument of periapsis of 60 deg. For lunar south pole observation, a 90 deg argument of periapsis is best, so this would fall in the middle of the observed ΔV range.

Next, because the lunar transfers analyzed for this study are to be used by a small satellite which will have a relatively low thrust propulsion system, finite burn transfers were analyzed to more correctly model the actual fuel mass requirements. As with the

impulsive burn optimizations, 18 and 90 deg inclination Earth orbits were used as the initial orbits for the transfers. First the behavior of the translunar injection burn with changing argument of perigee of the Earth orbit was analyzed for both Earth orbits. For both orbits, the TLI burn time showed an oscillating behavior with argument of perigee. Although there was a pattern, the variation of the required burn time for the 18 deg inclination orbit only varied by less than a minute from the minimum to maximum burn times. But the 90 deg inclination orbit showed a much larger variation. This is because, for the 90 deg inclination orbit, as the argument of perigee moves away from either the ascending or descending node of the orbit, the required declination for intercept of the Moon increases greatly. Once this required declination is greater than the inclination of the Moon's orbit, the transfer will not intercept the Moon at the apogee of the transfer orbit. Instead, the apogee of the transfer orbit must be greater than the Moon's orbit requiring a larger TLI burn.

Because of the low variation for the 18 deg inclination orbit, arbitrary arguments of perigee, 0, 90, 180 and 270 deg, were chosen for further study. Like the impulsive burn cases, transfers were completed to a candidate frozen orbit with varying lunar orbit inclination. The results were similar, showing little effect of inclination on the fuel requirements. For the four cases, the average final mass was 608 kg. This is an average of 68 kg less than the associated impulsive burn cases. Thus, the more realistic finite burn requires 68 kg more propellant than the impulsive burn simplification predicts. This result validated the assumption that the transfer maneuvers should not be assumed to be impulsive.

For the 90 deg inclination case, the Earth orbit AoP with the shortest TLI burn time in each range around 0 and 180 deg AoP was selected for detailed optimization, as well as the two endpoints of each range. The AoPs chosen were -45, 20, 45, 135, 160, and 225 deg. For these six cases, complete lunar transfers were optimized to the candidate frozen orbit. The two cases with the shortest TLI burns were the most fuel optimal of the six cases, while the endpoint cases were, as expected, less optimal as was expected. The average final mass of these six cases was 560 kg, with a range from 539 to 584 kg. Again these results show that transfers from the 90 deg inclination Earth orbit are less optimal than transfers from the 18 deg inclination orbit for the candidate lunar frozen orbit investigated.

The final analysis of this study was the optimization of phased multiple perigee burn transfers. By breaking the TLI burn into several smaller burns, gravity losses were decreased. Additionally the effect of increasing the thrust of the propulsion system from 100 N to 150 N was also analyzed. The initial phased transfer analyses raised the apogee of the Earth orbit to the semi-major axis of the Moon's orbit without actually intercepting the Moon. The four cases analyzed were 50-75-100-200-384, 50-100-200-384, 100-200-300-384, and 75-150-384 transfers, where each number is the new apogee in thousands of kilometers. For both thrust levels, the most fuel optimal transfer was the first which split the TLI burn into five separate transfers. The final mass for each of the thrust levels was 786 and 791 kg respectively. The least fuel optimal transfer was the 100-200-300-384 transfer. It resulted in a final mass of 737 kg for the 100 N thrust case and a mass of 777 kg for the 150 N case.

Phased transfers of three perigee burns and a lunar orbit insertion burn were then completed for each thrust case. These transfers were 50-100-Moon, 75-150-Moon, and 100-200-Moon. For the 100 N case, these resulted in final masses of 636, 638, and 609 kg respectively. While the 150 N thrust engine resulted in final masses of 651, 651, and 641 kg. Both thrust cases show that the third transfer was less fuel optimal, but the first two were comparable. The phased transfers reduced the fuel mass requirement over the single burn transfer by 22 to 51 kg for the 100 N case and 25 to 35 kg for the 150 N case.

Future Work

This study focused on the optimization of lunar transfers from an Earth orbit to a given lunar orbit. For these transfers, only the shape and inclination of the lunar orbit was targeted. The right ascension of the ascending node of the lunar orbit was free to be any value. Further research could be done to analyze the effect of right ascension of the ascending node on the fuel requirements of lunar transfers. Also, analyses could be completed on how varying the initial mass of the spacecraft affects the fuel requirements. Further optimization of the intermediate orbits used by a multiple-burn phased transfer is also suggested. Finally, since a constellation of navigation and communications spacecraft is likely to be required to meet the goals of the Vision for Space Exploration, research will also be necessary on the transfer and deployment of such a constellation.

REFERENCES

[1] Bush, G. W., "President Bush Announces New Vision for Space Exploration Program," *The White House* [website], URL: http://www.whitehouse.gov/news/releases/2004/01/20040114-3.html [cited 5 March 2008].

[2] Hill, C., "Magnolia-1 Small Satellite Program," Mississippi State University, 2006.

[3] Bate, R. R., Mueller, D. D., and White, J. E., *Fundamentals of Astrodynamics*, Dover Publications, New York, 1971, pp. 321-327.

[4] Kopal, Z., *The Moon*, D. Reidel, Dordrecht-Holland, 1969, pp. 5-7.

[5] Vallado, D. A., *Fundaments of Astrodynamics and Applications*, 2nd ed., Microcosm Press, El Segundo, 2004, pp. 310-319, 908.

[6] Konopliv, A. S., Asmar, S. W., Carranza, E., Sjogren, W. L., and Yuan, D. N., "Recent Gravity Models as a Result of the Lunar Prospector Mission," *Icarus*, Vol. 150, No. 1, 2001, pp. 1-18.

[7] Coolidge, L., Delaney, J., Lee, B., Rector, T., and Stuart, J., "The Next 20 Years-Can Small Sats Become a Mainstream Asset for the US Government," *2006 Small Satellite Conference*, Logan, UT, AIAA/USU, 2006, pp. 1-7.

[8] Underwood, C., "Spacecraft Systems Design," Surrey Satellite Technology Ltd, Guildford, UK, 10-14 Dec. 2007 (unpublished).

[9] Taylor, M., "Magnolia Requirements," Surrey Satellite Technology Ltd, Guildford, UK, 23 Nov. 2007 (unpublished).

[10] Isakowitz, S. J., Hopkins, J. B., and Hopkins Jr., J. P., *International Reference Guide to Space Launch Systems*, AIAA, Reston, VA, 2004, pp. 329-346.

[11] Ely, T. A., "Stable Constellations of Frozen Elliptical Inclined Lunar Orbits," *Journal of the Astronautical Sciences*, Vol, 53, No. 3, July-Sep. 2005, pp. 301-316.

[12] Miller, J. K., "Lunar Transfer Trajectory Design and the Four-Body Problem," *AAS/AIAA Space Flight Mechanics Meeting*, Vol. 114, AAS/AIAA, Ponce, Puerto Rico, 2003, pp. 685-695.

[13] "Magnolia Mission Options Review," Surrey Satellite Technology Ltd, Guildford, UK, 23-24 Oct. 2007 (unpublished).

[14] Racca, G.D., et al., "SMART-1 Mission Description and Development Status," *Planetary and Space Science*, Vol. 50, 2002, pp. 1323-1337.

[15] Ocampo, C., and Morcos, F., "Copernicus: User Reference Guide," *Copernicus Version 1.0* [CD-ROM]. 2006.

[16] Ocampo, C., "An Architecture for a Generalized Spacecraft Trajectory Design and Optimization System," *International Conference on Libration Point Orbits and Applications*, Aiguablava, Spain, 2002.

[17] Ocampo, C., "Finite Burn Modeling for a Generalized Spacecraft Trajectory Design and Optimization System," *Annals of the New York Academy of Sciences*, Vol. 1017, 2004, pp. 210-233.

[18] Gill, P. E., Murray, W., and Saunders, M. A., "User's Guide for Snopt version 6, A Fortran Package for Large-Scale Nonlinear Programming," 2002, pp. 3, 6-8.

[19] Rais-Rohani, M., "Handout #4: Mathematical Programming Methods for Constrained Optimization," ASE 4553 Engineering Design Optimization, Mississippi State University, 2007.

[20] Hill, P., and Peterson, C., *Mechanics and Thermodynamics of Propulsion*, 2nd ed., Addison-Wesley Publishing, New York, 1992, p. 473.